BBA - Molecular Basis of Disease 1863 (2017) 2904–2923

Contents lists available at ScienceDirect

BBA - Molecular Basis of Disease

journal homepage: www.elsevier.com/locate/bbadis

Berberine-induced cardioprotection and Sirt3 modulation in doxorubicin-treated H9c2 cardiomyoblasts

Ana R. Coelho[a,b,1], Tatiana R. Martins[a,1], Renata Couto[a,1], Cláudia Deus[a,b], Cláudia V. Pereira[a], Rui F. Simões[a], Albert A. Rizvanov[c], Filomena Silva[a], Teresa Cunha-Oliveira[a], Paulo J. Oliveira[a,*], Teresa L. Serafim[a]

[a] CNC - Center for Neuroscience and Cell Biology. University of Coimbra, UC Biotech Building, Lot 8A, Biocant Park, 3060-197 Cantanhede, Portugal
[b] IIIUC - Institute for Interdisciplinary Research, Casa Costa Alemão - Pólo II, Rua Dom Francisco de Lemos, 3030-789 Coimbra, Portugal
[c] Kazan Federal University, 18 Kremlyovskaya Street, Kazan 420008, Russian Federation

ARTICLE INFO

Keywords:
Doxorubicin
Berberine
Sirtuin 3
Cardiotoxicity

ABSTRACT

Doxorubicin (DOX) is one of the most widely used anti-neoplastic agents. However, treatment with DOX is associated with cumulative cardiotoxicity inducing progressive cardiomyocyte death. Sirtuin 3 (Sirt3), a mitochondrial deacetylase, regulates the activity of proteins involved in apoptosis, autophagy and metabolism. Our hypothesis is that pharmacological modulation by berberine (BER) pre-conditioning of Sirt3 protein levels decreases DOX-induced cardiotoxicity. Our results showed that DOX induces cell death in all experimental groups. Increase in Sirt3 content by transfection-mediated overexpression decreased DOX cytotoxicity, mostly by maintaining mitochondrial network integrity and reducing oxidative stress. p53 was upregulated by DOX, and appeared to be a direct target of Sirt3, suggesting that Sirt3-mediated protection against cell death could be related to this protein. BER pre-treatment increased Sirt3 and Sirt1 protein levels in the presence of DOX and inhibited DOX-induced caspase 9 and 3-like activation. Moreover, BER modulated autophagy in DOX-treated H9c2 cardiomyoblasts. Interestingly, mitochondrial biogenesis markers were upregulated in in BER/DOX-treated cells. Sirt3 over-expression contributes to decrease DOX cytotoxicity on H9c2 cardiomyoblasts, while BER can be used as a modulator of Sirtuin function and cell quality control pathways to decrease DOX toxicity.

1. Introduction

The anthracycline Doxorubicin (DOX) is one of the most prescribed and effective anti-cancer agents [1,2]. The clinical use of DOX has been associated with a cumulative and dose-specific cardiotoxicity that involves the development of congestive heart failure [3–6]. Being a very potent chemotherapeutic, a more effective prevention of DOX-induced cardiotoxicity is needed in order to potentially optimize the effective dosage given to patients and therefore reduce morbidity.

Adult cardiac progenitor cells (CPCs), present in adult heart, contain stem cell characteristics and are involved in tissue homeostasis and myocardial regeneration during pathological conditions [7–9]. CPCs have been studied in the context of several pathological conditions in animal and humans including as a pathophysiological target against DOX cardiotoxicity [9–12]. One relevant model to investigate DOX-induced effects on CPCs is the H9c2 cell line, which has morphological characteristics similar to immature embryonic cardiomyocytes [2,13–16].

It has been previously described that DOX, at 0.5 and 1 μM concentrations, equivalent to those achieved in the plasma upon administration of therapeutic doses [14], promotes metabolic stress and increases protein acetylation of crucial mitochondrial enzymes [17–19]. Sirtuins are NAD^+-dependent deacetylases that catalyse the deacetylation of histone and non-histone lysine residues, also having protein ADP-Ribosyltransferase activity [20]. Sirtuin 3 (Sirt3) is the major mitochondrial deacetylase [21], modulating several mitochondrial pathways [22]. Sirt3 is involved in the maintenance of oxidative phosphorylation during stress, regulation of ROS generation at the electron transport chain (ETC), as well as detoxification of ROS via activation of antioxidant enzymes, such as glutathione and superoxide dismutase 2 (SOD2) [17,23–25]. Moreover, it was shown that Sirt3 was capable of deacetylating OPA1, contributed to the preservation of

* Corresponding author.
E-mail addresses: ana.coelho@uc-biotech.pt (A.R. Coelho), tmartins@itqb.unl.pt (T.R. Martins), Renata.Couto@med.uni-goettingen.de (R. Couto), cmcdeus@cnc.uc.pt (C. Deus), claudia.pereira@med.miami.edu (C.V. Pereira), rui.simoes@uc-biotech.pt (R.F. Simões), albert.rizvanov@kpfu.ru (A.A. Rizvanov), filomena.silva@uc-biotech.pt (F. Silva), teresa.oliveira@uc-biotech.pt (T. Cunha-Oliveira), pauloliv@cnc.uc.pt (P.J. Oliveira), tserafim@medicina.ulisboa.pt (T.L. Serafim).
[1] Authors contributed equally.

http://dx.doi.org/10.1016/j.bbadis.2017.07.030
Received 2 February 2017; Received in revised form 18 July 2017; Accepted 27 July 2017
Available online 29 July 2017
0925-4439/

mitochondrial network structure, and protection of cardiomyocytes from DOX-mediated cell death [19]. Altogether, these evidences indicate that Sirt3-regulated pathways may be a potential target to preserve cardiac mitochondrial function and the overall contractile function [26,27].

Novel therapeutic approaches based on combined treatments with antioxidants have been developed to decrease side effects. One of such molecules is berberine (BER), a natural compound used in traditional Chinese medicine. Among the many biological actions described for BER, antitumoral/antiproliferative [28–30], antioxidant [31], and antiarrhythmic [32] are the most relevant. The beneficial potential of BER includes cardioprotective effects [32–34], since it was able to reduce ventricular afterload and augment myocardial contractibility [33,34]. On the other hand, BER also increases Sirt3 activity which results in the activation of mitochondrial biogenesis pathways and increased mitochondrial capacity [35,36].

Taking this into account, our hypothesis is that BER modulation of Sirt3 levels inhibits DOX-induced mitochondrial dysfunction in H9c2 cardiomyoblasts. This modulation of protective mechanisms will allow the control of DOX toxicity, as well as the regulation of mitochondrial metabolism, oxidative stress and cell death.

2. Materials and methods

2.1. Reagents

Dulbecco's modified Eagle's medium (DMEM), fetal bovine serum (FBS), Penicillin Streptomycin, ethylenediaminetetraacetic acid (EDTA), 0.05% Trypsin-EDTA, 1 × Opti-MEM Reduced Serum Medium were received from Invitrogen (Carlsbad, CA, USA). DOX, Sulforhodamine B (SRB), protease inhibitor cocktail (PMSF), bovine serum albumin (BSA), ammonium persulfate (APS), Bradford reagent, calcium chloride ($CaCl_2$), β-mercaptoethanol, sodium dodecyl sulfate (SDS) and trypan-blue were obtained from Sigma-Aldrich (St. Louis, MO, USA). Other chemical reagents were also purchased from Sigma-Aldrich, including those necessary to prepare 1 × Phosphate Buffered Saline (PBS). Cell lysis buffer was obtained from Cell Signaling (Danvers, MA, USA). Acrylamide, Laemmli buffer, polyvinylidene difluoride membrane (PVDF) membranes and *N,N,N′,N′* Tetramethyllenediamine (TEMED) were from BioRad (Hercules, CA, USA). The Enhanced ChemiFluorescence (ECF) detection system was obtained from Healthcare Life Sciences (Buckinghamshire, UK). Acetic acid and ethanol were obtained from Merck Millipore (Whitehouse Station, NJ, USA). All reagents and chemical compounds used were the greatest degree of purity commercially available. In the preparation of every solution, ultrapure distilled water filtered by the Milli Q from Millipore (Whitehouse Station, NJ, USA) system was always used.

2.2. Cell culture and cell treatments

H9c2 cell line (catalogue number CRL1446TM) was purchased from American Type Cell Culture (ATCC, Manassas, VA). The cells were grown in DMEM supplemented with 10% FBS, 1.5 g/L sodium bicarbonate and 1% of penicillin-streptomycin plus amphotericin B in 100 mm cell culture dishes at 37 °C in a humidified atmosphere of 5% CO_2. Cells were fed every 2–3 days and sub-cultured once they reached approximately 80% confluence in order to prevent cell differentiation, and were used between passages 7 and 20. For quantitative real-time PCR (qRT-PCR), Western Blot (WB), and caspase-like activity, cells were seeded at a density of 50,000 cells per mL for control and 85,000 cells per mL for the other conditions in 55 cm^2 culture dishes and cultured for one day. Then, cells were transfected and 24 h later compounds were added. For the other assays, such as SRB, flow cytometry and fluorescence microscopy, cells were seeded in order to reach a density of 60-70% in next day, to be transfected. Twenty-four hours after transfection, cell seeding was performed at a density of 10,000 cells per mL in 24-well plates for SRB; 20,000 cells per mL in six-well plates with 18 × 18 mm coverslip for microscopy and 40,000 cells per mL in 6 multiwell for flow cytometry. Two concentrations of DOX, which are usually present in plasma of patients treated with DOX (0.5 and 1 μM), were directly added to culture media. After 24 h post-treatment, cells were collected and stored at − 80 °C or were used to the assays. Two concentrations of BER (1 and 10 μM) were used for 72 h with solutions prepared in DMSO (also used as the vehicle in control groups) and added to the culture media. Both BER concentrations were previously selected using cell mass and caspase 3 and 9 like-activity assays. Viable cell counting for cell seeding was performed by using Trypan Blue exclusion method.

2.3. Transformation of competent cells and plasmid purification

One Shot TOP10 Chemically Competent E.coli (Invitrogen) was used to transform cells for high-efficiency cloning and plasmid propagation, according to the manufacturer's protocol. Following transformation procedure, cells were harvested by centrifugation at 6000 × *g* for 15 min at 4 °C and the pellet was collected. After, plasmid purification was performed using Hispeed Plasmid Midi Kit (Qiagen, Valencia, CA) by following the manufacturer's protocol. The DNA concentration was determined with a Nanodrop spectrophotometer (Thermo Scientific, Lanham, MD).

2.4. Sirt3 gene overexpression in H9c2 cells

To evaluate the role of Sirt3 in DOX toxicity on H9c2 cardiomyoblasts, the wild-type (hSirt3-Flag) and the empty vector (Control) were obtained with the above procedure and were overexpressed in these cells [37]. Sirt3 overexpression was performed using the murine Long Form as described in [38]. In order to form the complexes of DNA, a 1:3 ratio of 9 μg of DNA and XtremeGENE HP DNA Transfection Reagent (Roche, Mannheim, Germany) were used in Opti-MEM I Reduced Serum Medium, for 15 min. Afterwards, the transfection was performed and cells were incubated in growth medium for 24 h, to obtain a transient protein transfection. Besides the three groups described above, one control condition was performed by using transfection reagent only.

2.5. Sulforhodamine B colorimetric assay

The SRB assay (Vichai and Kirtikara 2006) was used to measure cell mass indirectly through determination of the total cell protein. After treatment, the incubation media was removed, and cells were fixed in 1% acetic acid in ice-cold methanol overnight at − 20 °C. Cells were then incubated with 0.05% (w/v) SRB for 1 h at 37 °C. Subsequently, SRB was removed and wells were washed with 1% acetic acid to remove unbound stain. Dye bound to cell proteins was extracted with 10 mM Tris-base solution, pH 10, and its absorbance was read at 540 nm in a VICTOR × 3 Microplate Reader (Perkin Elmer, Waltham, MA, USA).

2.6. Collection of total protein

In order to obtain total cellular extracts, cells grown in 55 cm^2 culture dishes were harvested by trypsinization and washed once with PBS. Floating cells were also collected and combined with adherent cells. In order to collect all cells, two centrifugation steps were performed for 5 min at 1000 × *g*. Before protein quantification, the cellular pellet was resuspended in cell lysis buffer supplemented with PMSF, a protease inhibitor, and samples were then sonicated. Protein was quantified by the Bradford assay (Bradford, 1976), using BSA as standard.

2.7. Western blot analysis

After denaturation at 95 °C or 50 °C for OXPHOS cocktail antibody, for 5 min in a 2× Laemmli sample loading buffer (Bio-Rad), an equivalent amount of protein (40 μg) was separated in 9%, 10%, 12% or 14% polyacrylamide gel electrophoresis and electrophoretically transferred to a PVDF membrane. After membrane blocking with 5% milk (Bio-Rad) in Tris-Buffered Saline Tween (TBS-T; 50 Tris-HCl, pH 8; 154 mM NaCl and 0.1% Tween 20) for 2 h at room temperature under continuous stirring, membranes were incubated overnight at 4 °C, under stirring, with the antibodies directed against Caspase 3 (1:1000, Cell Signaling, rabbit), Caspase 9 (1:750, Cell Signaling, rabbit), OXPHOS (1:1000, MitoScience, mouse), p53 (1:1000, Cell Signaling, mouse), Sirt3 (1:1000; Cell Signaling, rabbit), Acetyl anti-SOD2 (K68) and Anti-SOD2/MnSOD (1:750, Abcam, rabbit), Tom20 (1:1000, Santa Cruz, rabbit), p62 (1:1000, MBL, rabbit), Mitochondrial Transcription Factor A (Tfam) (1:500, Santa Cruz, goat) LC-3 I/II (1:100, MBL, rabbit). Once incubation was complete, membranes were incubated with alkaline phosphatase conjugated secondary antibodies (1:2500) for 1 h at room temperature under continuous agitation. Membranes were washed again and incubated with ECF system (from GE Healthcare, Piscataway, NJ), for 5 min maximum at room temperature. Fluorescence was read using the UVP Biospectrum 500 Imaging System (UVP, LLC, Cambridge, UK) through UV epi-illumination (365 nm). Before blocking, the membranes were stained with Ponceau S reagent to confirm equal protein loading in each membrane [39]. Band density was measured by using VisionWorks Analysis Software (UVP).

2.8. Cell death analysis by flow cytometry

To evaluate cell death, transfected cells were harvested by trypsinization and resuspended in buffer medium (120 mM NaCl, 3.5 mM KCl, 0.4 mM KH_2PO_4, 20 mM HEPES, 5 mM $NaHCO_3$, 1.2 mM $NaSO_4$, 10 mM sodium pyruvate at pH 7.4) supplemented with 1.2 mM $MgCl_2$, 1.3 mM $CaCl_2$. Next, a set of cells was incubated with 100 nM Sytox Green and another with 800 nM Calcein-AM. These probes give information about dead and live cells, respectively. Two samples of non-labelled cells, with and without DOX, were also analyzed to calibrate the FACSCalibur Flow Cytometer system (BD Biosciences, San Jose, California, USA), taking cell auto-fluorescence and DOX fluorescence into account. Samples were kept on ice until use and 8000 cells were analyzed on a FACSCalibur Flow Cytometer. Data was analyzed using CellQuest Pro Software Package Cytometer (BD Biosciences, San Jose, California, USA).

2.9. Vital labeling of H9c2 mitochondria with tetramethylrhodamine, methyl ester (TMRM) and visualization by epifluorescence microscopy

To indirectly assess mitochondrial transmembrane electric potential ($\Delta\psi_m$), cells were seeded on coverslips in six-well plates as described above. Before the assay, cells were rinsed with PBS 1× and incubated in buffer medium (described in Section 2.8) with $TMRM^+$ (100 nM) and with Hoechst 33342 (1 μg/mL) for 30 min. After incubation, coverslips were removed from the wells and placed inverted on slides. All images were obtained with Nikon Eclipse Ti-S (Nikon Instruments Inc., NY, USA). Cells were analysed in terms of their mean and S.D. values for the fluorescence of each cell using ImageJ software.

2.10. Vital epifluorescence microscopy of H9c2 cells labeled with Mitosox Red and MitoTracker Green

H9c2 cells were seeded on coverslips in six-well plates and treated as described above. Afterwards, on the day of the assay, cells were rinsed with PBS 1× and incubated in buffer medium (described in Section 2.9) with MitoSox Red (5 μM) and the mitochondrial probe MitoTracker Green (200 nm) for 30 min. Rotenone (250 μM), a complex I inhibitor, was used as a positive control to increase superoxide anion detection. Cells were imaged by epifluorescence microscopy by using a Nikon Eclipse Ti-S (Nikon Instruments Inc., NY, USA).

2.11. Caspase-like activity assay

Caspase 3 activation was measured with two different methodologies. In order to measure caspase 3/7- like enzymatic activity, the Caspase-Glo 3/7 was used. Cells were seeded in 96 multiwell plates and the kit was used at the end of the cell treatment. The second method involved measurement of caspases −3 and −9 like activities separately. After transfection and DOX treatment, H9c2 cells were harvested by trypsinization and washed once with PBS. To collect total cells, two centrifugation steps were performed for 5 min at 1000 × *g*. Floating cells were also collected and combined with adherent cells. Cellular pellets were resuspended in cell lysis buffer supplemented with PMSF, and kept at −80 °C until used. Protein content was assayed by the Bradford method [40], using BSA as standard. To measure caspase-3- and caspase 9-like activity, aliquots of cell extracts containing 25 μg (for caspase 3) or 50 μg (for caspase 9) total protein were incubated in a reaction buffer containing 25 mM HEPES (pH 7.4), 10% sucrose, 10 mM dithiothreitol (DTT), 0.1% 3[(3-cholamidopropyl)dimethylammonio]-propanesulfonic acid, and 100 μM caspase substrate (Ac-DEVD-*p*-nitroanilide (pNA) for caspase 3 or Ac-LEHD-pNA for caspase 9) for 2 h at 37 °C. Caspase-like activities were determined by following the detection of the chromophore pNA after cleavage from the labeled substrate Ac-DEVD-pNA or Ac-LEHD-pNA. The method was calibrated with known concentrations of pNA.

2.12. Cathepsin B and D-like activity assay

The evaluation of lysosomes viability was performed by measuring cathepsin B and D-like activities. Cathepsin B and D like-activities were measured by fluorimetric and spectrophotometric detection, respectively [41,42]. H9c2 cells were cultured as previously described. After cell treatment, the culture medium was collected and 3 mL of extraction buffer (PBS 1 × supplemented with 0.1 g/L EDTA) were added to each dish. Cells were then scraped and the cell suspension was collected and added to the correspondent culture medium. Cell suspensions were centrifuged at 340 xg for 4 min, the pellet was collected and washed with PBS 1 × and centrifuged again at 340 × *g* for 4 min. Pellets were resuspended in 200 μL of lysis buffer (50 mM HEPES pH 7.4, 100 mM NaCl, 0.1% (wt/vol) CHAPS, 0.1 mM EDTA and 10 mM DTT). The cell suspensions were kept at −80 °C until used. The protein content was quantified by the Bradford method [40], using BSA as standard. For Cathepsin B-like activity determination, aliquots of 50 μL of each sample were incubated with 40 μM of Z- Arg- Arg-*N*-methyl-coumarin (C5429, Sigma- Aldrich, St. Louis, MO, USA) in incubation buffer (100 mM sodium acetate pH 5.5, 1 mM EDTA, 5 mM DTT and 0.1% (vol/vol) Brij-35) at 37 °C for 20 min. After the incubation, 150 μL of stopping buffer (33 mM sodium acetate pH 4.3, 33 mM sodium chloroacetate) were used to stop the enzymatic reaction. Cathepsin B like-activity was determined by the detection of the *N*-methyl-coumarin (A9891, Sigma-Aldrich, St. Louis, MO, USA) fluorometrically at 360 nm excitation and 460 nm emission in VICTOR ×3 (Perkin Elmer, Inc.) reader. The method was calibrated with known concentrations of *N*-methyl-coumarin. For Cathepsin D like-activity determination, aliquots of 75 μL of each sample were incubated with 125 μL of 3% (wt/vol) Hemoglobin (H2625, Sigma-Aldrich, St. Louis, MO, USA) in 200 mM acetic acid at 37 °C for 30 min. After the incubation, 125 μL of 15% (vol/vol) TCA was added to the samples and they were kept at 4 °C for 30 min. Samples were then centrifuged at 13,400 × *g* for 5 min. Cathepsin D-like activity was determined by the measurement of optic density of 200 μL supernatant at 280 nm in a Cytation 3 (BioTek Instruments, Inc., Winooski, USA) multiplate reader.

2.13. Statistical analysis

Data are expressed as mean ± SEM for the number of experiments indicated in the figure legends. To evaluate the transfection effect and treatment, a two-way analysis of variance (ANOVA) followed by the Tukey multiple comparison test was applied. To compare the effect of DOX in control cells, a one-way ANOVA followed by the Tukey post-test was used. For the evaluation of BER effect in DOX-induced cardiotoxicity studies, One-way ANOVA was used followed by the Dunett or Bonferroni post-test for multiple comparisons. Statistical analysis was performed in comparison with the control (untreated cells) or between groups, as described in figure legends. Significance was accepted when $p < 0.05$.

3. Results

3.1. Sirt3 overexpression protects against mitochondrial fragmentation and oxidative stress induced by DOX

In order to test our hypothesis, we initially analysed basal Sirt3 content on H9c2 cells. We confirmed by WB whether Sirt3 overexpression (hSirt3; Fig. S1) was effective, before evaluating DOX cytotoxicity under the different experimental conditions.

Our group has previously demonstrated that at low concentrations, DOX causes mitochondrial depolarization on H9c2 cells [14]. In this sense, we studied the effect of Sirt3 overexpression on mitochondrial depolarization by vital epifluorescence microscopy using the fluorescent dye $TMRM^+$ (Fig. 1). In control cells, transfected with an empty vector, mitochondrial fragmentation was also observed after DOX treatment. Sirt3 overexpression resulted in mitochondrial elongation (Fig. 1B) and polarization (Fig. 1C), especially with 1 μM DOX. Since DOX-induced oxidative stress on cardiac cells has been implicated as one of the major mechanisms responsible for cardiotoxicity [14], we used MitoSox Red, a dye which evaluates the presence of mitochondrial superoxide anion. H9c2 cells overexpressing Sirt3 and treated with DOX were dual-labelled with MitoTracker Green, which labels mitochondria regardless of the polarization state and MitoSox Red (Fig. 2). The images obtained by epifluorescence microscopy showed that Sirt3 overexpression appeared to prevent the increase in mitochondrial superoxide anion after DOX treatment, with a stronger red fluorescence in the control-1 μM DOX comparatively to hSirt3-1 μM DOX condition. Due to the fact DOX also emits fluorescence in the red channel and is seen in the nuclear areas, it was not possible to quantify mean cellular MitoSox Red fluorescence. In order to overcome this issue, we measured total and acetyl protein form of the major enzymatic superoxide anion scavenger in the mitochondrial matrix, manganese superoxide dismutase (SOD2) by Western blot (see later Fig. 9).

3.2. Sirt3 potentiates DOX-induced overexpression of several mitochondrial OXPHOS subunits

DOX cardiotoxicity involves disturbances of heart mitochondrial function and bioenergetics [6]. We next investigated the potential role of Sirt3 on DOX-effects on the mitochondrial oxidative phosphorylation (OXPHOS) machinery. The protein content of OXPHOS subunits was assessed by WB using an OXPHOS antibody cocktail (Fig. 3). Since Sirt3 regulates mitochondrial substrate oxidation and ATP production under basal conditions [43], as well as protein synthesis by deacetylating the mitochondrial ribosomal protein L10 [44], we next tested whether modulating Sirt3 levels in H9c2 cells would result in OXPHOS protein alterations after DOX treatment. Contrarily to what was expected, hSirt3 did not produce any difference on regarding OXPHOS protein content in cells treated with 1 μM concentration of DOX (Fig. 3). Interestingly, for a lower concentration of DOX (0.5 μM) mitochondrial complex I and III subunits were significantly increased in the hSirt3/DOX group when compared to the same condition in the absence of DOX (Fig. 3C and G). A similar trend, but with no statistical significance, was visible on SDHB (complex II) and ATP5A (complex V) subunits (Fig. 3E and I).

3.3. Sirt3 overexpression protects H9c2 cells against DOX-induced cell death

Multiple forms of cell death, such as apoptosis, necrosis and autophagy, can be triggered by mitochondrial dysfunction, namely increased oxidative stress or even disruption on OXPHOS machinery [45]. We initially measured H9c2 cell mass alterations after Sirt3 manipulation, as well as 24 h after treatment with 0.5 and 1 μM of DOX by using the colorimetric SRB technique. Both DOX concentrations induced a significant decrease of H9c2 cardiomyoblast mass. The results also showed that the overexpression of Sirt3 had no effect on the decreased cell mass caused by DOX treatment (Fig. S2). Based on these results, we decided to continue the subsequent experiments by using 1 μM DOX.

Since the SRB method does not allow to distinguish between cell death and cell proliferation, we next evaluated the proportion of dead and live cells by using Sytox green and Calcein-AM fluorescent dye, respectively, by flow cytometry (Fig. 4) [46]. Although not statistically significant, the results showed an increase in the number of live cells following Sirt3 overexpression (Fig. 4A). Cell death was then confirmed by using the MultiTox-Glo multiplex cytotoxicity assay (Fig. 4B). H9c2 cell death increased after treatment with 1 μM DOX. This assay confirmed the protection conferred by Sirt3 on DOX cytotoxicity, since Sirt3 overexpression partially prevented cell death when compared to DOX-treated cells.

Cardiomyocytes apoptosis, by caspase-dependent and independent mechanisms, has been proposed to mediate DOX-induced deterioration of cardiac function, with mitochondria playing a key role [14,16,47]. Afterwards, we measured protein content and activity of the initiator caspases 8 and 9, and the effector caspase 3, all involved in the apoptotic process. Caspase 8, a key component of the extrinsic pathway, was not significantly altered in any of the experimental groups tested (data not shown). Sirt3 overexpression did not affect protein expression of caspase-9 (Fig. 5). Caspase 9-like activity was also measured by a colorimetric assay and the results showed a significant increase in caspase 9-like activity in control cells after treatment with 1 μM DOX, as expected. However, a significant decrease in caspase 9-like activity was observed in hSirt3 cells after the same treatment (Fig. 5E). Moreover, cleaved caspase 3 showed a large increase in the 1 μM DOX treatment group, and a significant decrease was observed with Sirt3 overexpression (Fig. 6C). In order to confirm the results obtained by WB, we evaluated caspase 3/7 activity after Sirt3 transfection and DOX treatment. We observed an increase in caspase 3/7 activity after treatment with 1 μM DOX which was decreased after overexpression of Sirt3 (Fig. 6D).

Taking into account previous results from our group and others [13,48–50], we next evaluated p53 protein content (Fig. 7A), a transcription factor which is overexpressed after DOX treatment. As expected, control cells showed a significant increase in p53 protein after treatment with 1 μM DOX (Fig. 7B). When cells were treated with 1 μM DOX a significant decrease of p53 protein content was observed in hSirt3 transfected cells (Fig. 7B). Once more, we observed a protective effect of Sirt3 overexpression on H9c2 cells.

3.4. Berberine induces Sirt3 overexpression, SOD2 activity, and decreases cytotoxicity in H9c2 cells

After validation of Sirt3 protective effects against DOX cardiotoxicity, pharmacological modulation of this deacetylase as therapeutic approach was tested. BER is a natural product described to induce Sirt3 activity *in vivo* [36]. Taking into account that Sirt1 also regulates mitochondrial biogenesis and metabolism [35], we next evaluated if BER

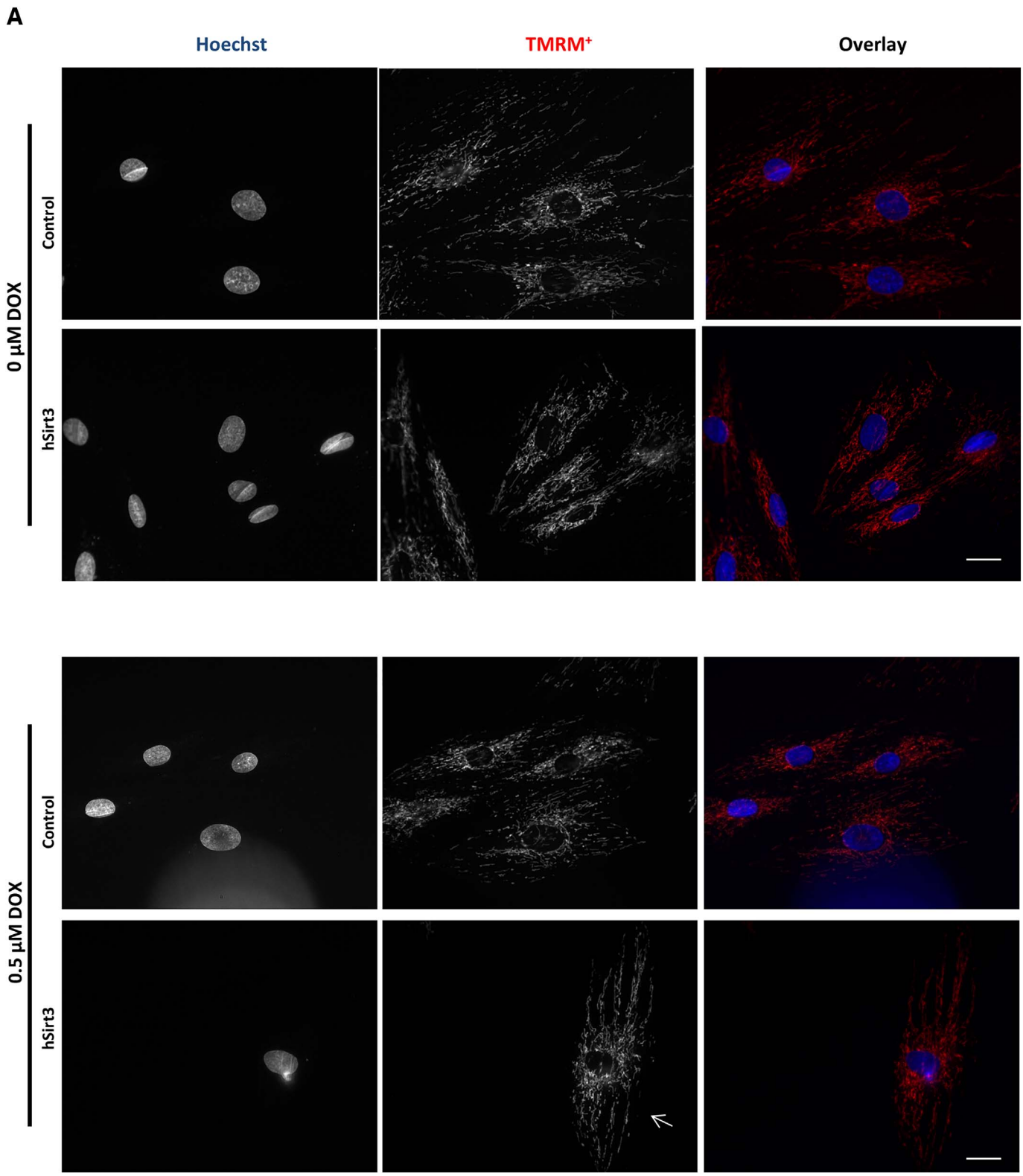

Fig. 1. Modulation of Sirt3 expression levels on DOX-induced mitochondrial depolarization in H9c2 cardiomyoblasts. H9c2 cardiomyoblasts were subjected to Sirt3 overexpression (hSirt3) and respective control condition, and incubated with DOX (0, 0.5 and 1 µM) for 24 h. **A)** Mitochondrial distribution and transmembrane electric potential were evaluated after $TMRM^+$ labelling (red fluorescence). Nuclear morphology was also analysed by labelling with Hoechst 33342 (blue fluorescence). Epifluorescence microscopy images were acquired by using a 40 × objective; all the panels are the same magnification. White bar, 20 µm. B) Quantification of mitochondrial elongation and C) cells fluorescence was analyzed in terms of their mean values (TMRM fluorescence) and also in terms of the fluorescence S.D. values of each cell. Data are presented as mean ± SD; n = 4 (seven to 20 cells per cover glass).

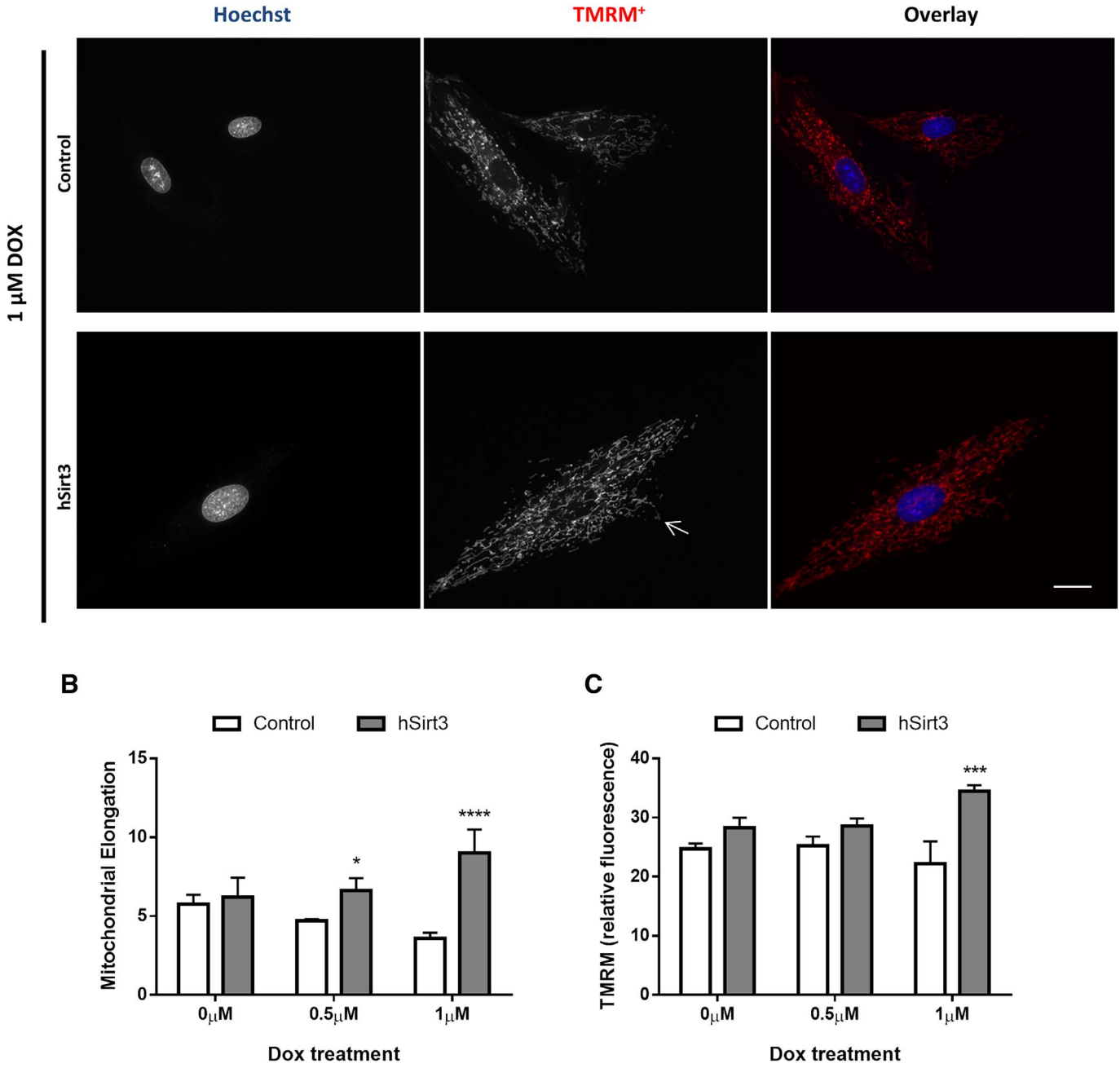

Fig. 1. (*continued*)

could affect the levels of both of these sirtuins in our cell model.

In this part of the study, different concentrations of BER were tested (from 1 μM to 100 μM) with the lowest concentrations having minimal effects on H9c2 cell mass (Fig. S3A). To determine the best BER concentration for subsequent studies cytotoxicity of BER *per se* was evaluated in terms of cell mass (Fig. S3B) and caspase activation (Fig. 8). Based in our results, 1 and 10 μM of BER were selected and H9c2 cells were initially pre-treated for 72 h followed the addition of 1 or 20 μM DOX, in the last 24 h. Lower DOX concentration (1 μM) was equivalent to those achieved in plasma after administration of therapeutic doses of DOX and the higher concentration (20 μM) was meant to mimic a single acute treatment [14].

The effect of combined BER/DOX treatments in sirtuin levels and caspase-like activity in H9c2 cells is represented in Fig. 8. Our results showed that treatment with 1 μM DOX alone resulted in slight increase of Sirt3 protein content (Fig. 8A). In addition, pre-treatment with 10 μM BER followed by 1 μM DOX resulted in a further increase in Sirt3 content when compared with the control (Fig. 8A, C). Regarding Sirt1, a similar pattern was observed (Fig. 8B). The combination of 10 μM BER with 1 μM DOX also led to an increase in the Sirt1 protein content when compared to 1 μM DOX alone (Fig. 8B, D). Our next step was to evaluate the effect of BER on DOX-induced caspase-like activity using a range of BER (0, 1 and 10 μM) and DOX (0, 0.5, 1 and 20 μM) concentrations (Fig. 8E, F). BER treatment *per se* did not significantly increase caspase 9 and 3-like activities (Fig. 8E, F). Our data (Figs. 5 and 6) and previous results from our laboratory [14] showed that DOX treatment (0.5, 1 and 20 μM) increased both caspase − 3 and − 9-like activities in H9c2 cells. The combination of 10 μM BER with 0.5 μM DOX resulted in a decrease in caspase 9-like activity when compared with 1 μM DOX alone (Fig. 8E). Pre-treatment with 1 μM BER statistically prevented caspase-9 activation induced by 1 μM DOX (Fig. 8E). Furthermore, pre-treatment with 10 μM BER also decreased caspase-9-like activity induced by 20 μM DOX, in comparison with 20 μM DOX alone (Fig. 8E). On the other hand, pre-treatment with 10 μM BER prevented caspase 3

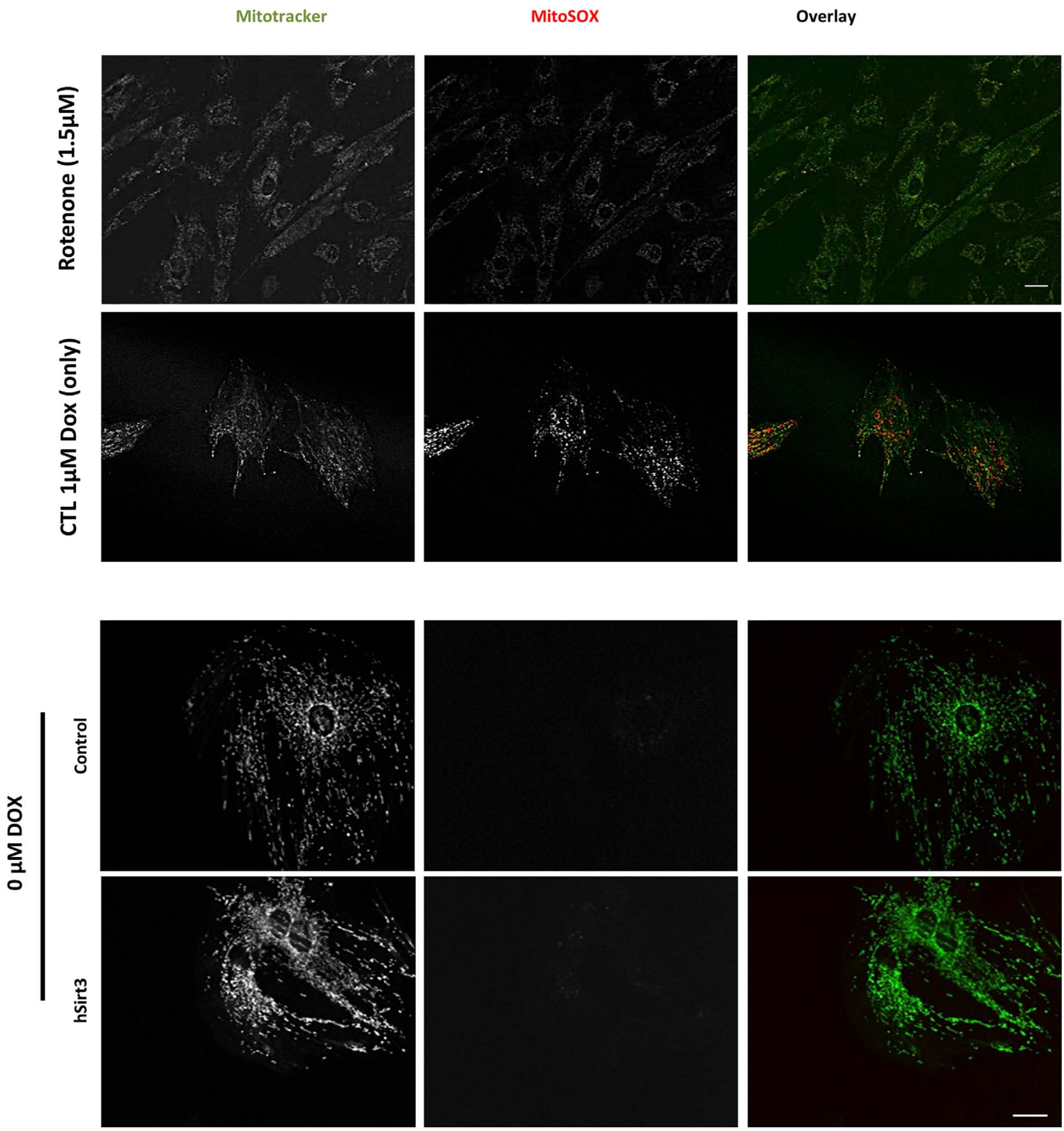

Fig. 2. Impact of Sirt3 overexpression on DOX-induced increase in mitochondrial superoxide anion in H9c2 cardiomyoblasts. H9c2 cardiomyoblasts were subjected to Sirt3 overexpression protocol and respective control conditions, and treated with DOX (0, 0.5 and 1 μM) for 24 h. Mitochondrial superoxide anion levels were evaluated using MitoSOX Red probe, and mitochondria were stained with MitoTracker Green to allow visualization of the mitochondrial network. Images were acquired by fluorescence microscopy using a 40 × objective. The cells were transfected with PcDNA only (control) or with human Sirt3 cDNA (hSirt3). We also used 1.5 μM Rotenone to increase generation of mitochondrial superoxide anion as a positive control, as well as cells treated only with DOX as control. Data represents 3 independent experiments. Scale bar of Rotenone panel represents 15 μm, all the others represents 20 μm.

activation induced by 1 or 20 μM DOX (Fig. 8F). For the lowest concentration (1 μM), BER pre-treatment was also able to prevent caspase-3 activation induced by 1 or 20 μM DOX (Fig. 8F).

We also measured total and deacetylated SOD2 protein content and we observed that total SOD2 is only increased when treated with BER (Fig. 9). By measuring the SOD2 acetylated/SOD2 total ratio, a decrease in SOD2 acetylated form in hSirt3/BER cells, was observed, which was increased when combined with DOX treatment (Fig. 9).

3.5. BER modulates autophagy in DOX-treated H9c2 cardiomyoblasts

Cardiac cells can eliminate damaged biomolecules and organelles through the activation of self-recycling pathways including autophagy. Cardiomyocytes can use autophagy as well as survival mechanism after

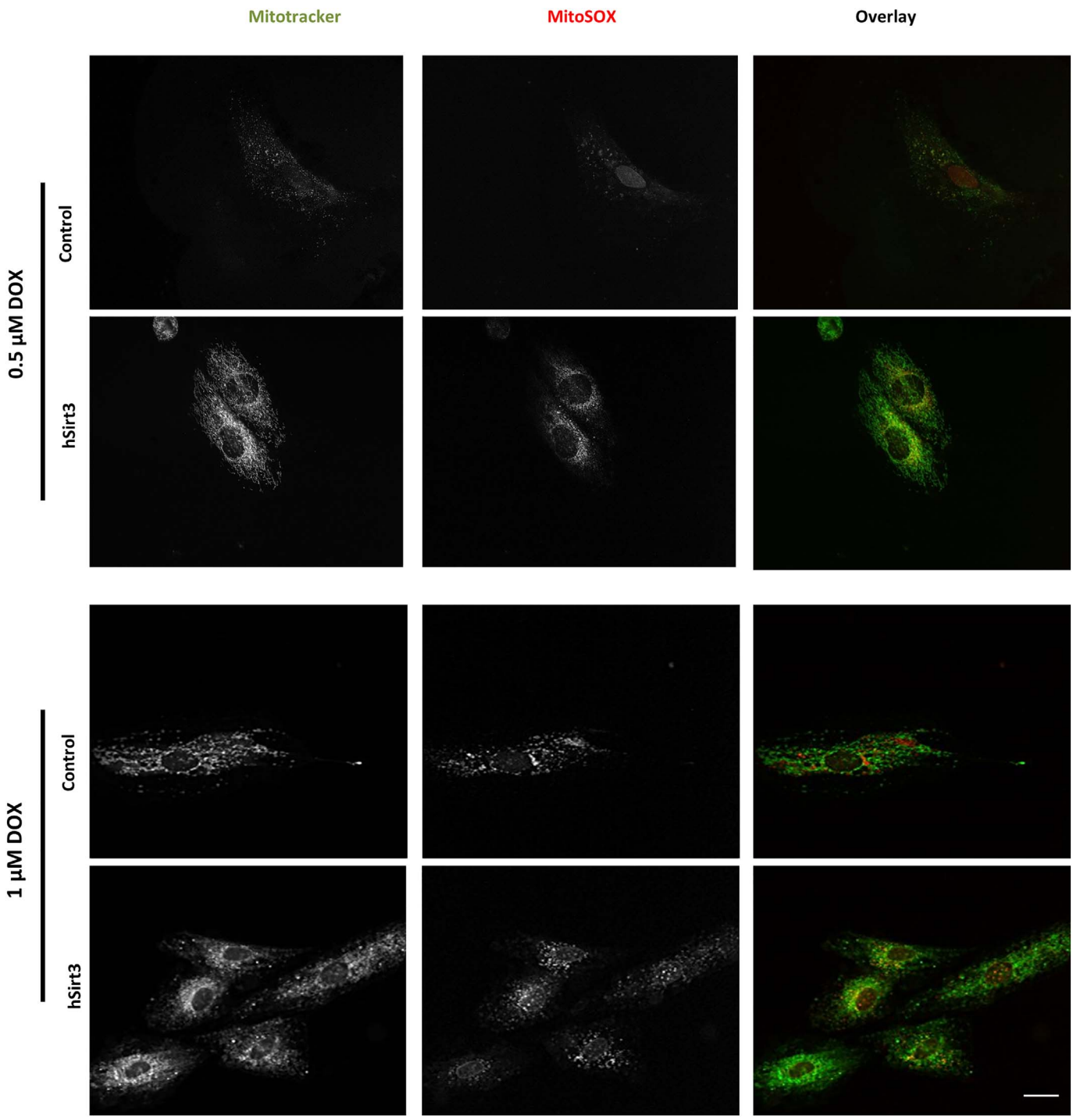

Fig. 2. (*continued*)

a stress stimulus, such as DOX treatment, managing the damage and restore energy homeostasis [51–53]. In fact, our data showed that 20 µM DOX increased LC3-I protein levels, while LC3-II protein levels were not altered in cells treated only with DOX. BER *per se* did not induce any alterations in the LC3-I -LC3-II conversion when compared with untreated cells (Fig. 10C,D). BER pre-treatment in H9c2 cells exposed to 1 µM DOX apparently increased the LC3-II content, although this result was not statistically significant. BER pre-treatment increased the LC3-II protein band in cells treated with 20 µM DOX, and appeared to increase the conversion of LC3-I into LC3-II in comparison within cells treated only with 20 µM DOX (Fig. 10A-D).

As p62/SQSTM1 binds directly to LC3 proteins during the autophagic pathway and accumulates when autophagy is inhibited, giving information about the autophagic flux [54]. We next evaluated the effect of BER in p62 protein content in DOX-treated H9c2 cells (Fig. 10E). Our results showed that DOX did not significantly affect p62 protein levels, although a tendency for a down-regulation of this protein was noticed. BER pre-treatment induced an increase in p62 protein content only in cells treated with DOX (1 and 20 µM), when compared to the respective DOX treatment alone. The increase in p62 protein observed in cells pre-treated with BER and exposed to 1 µM of DOX was also statistically significant when compared to control cells in the absence of BER.

Lysosomal viability is associated with high cathepsin B and low

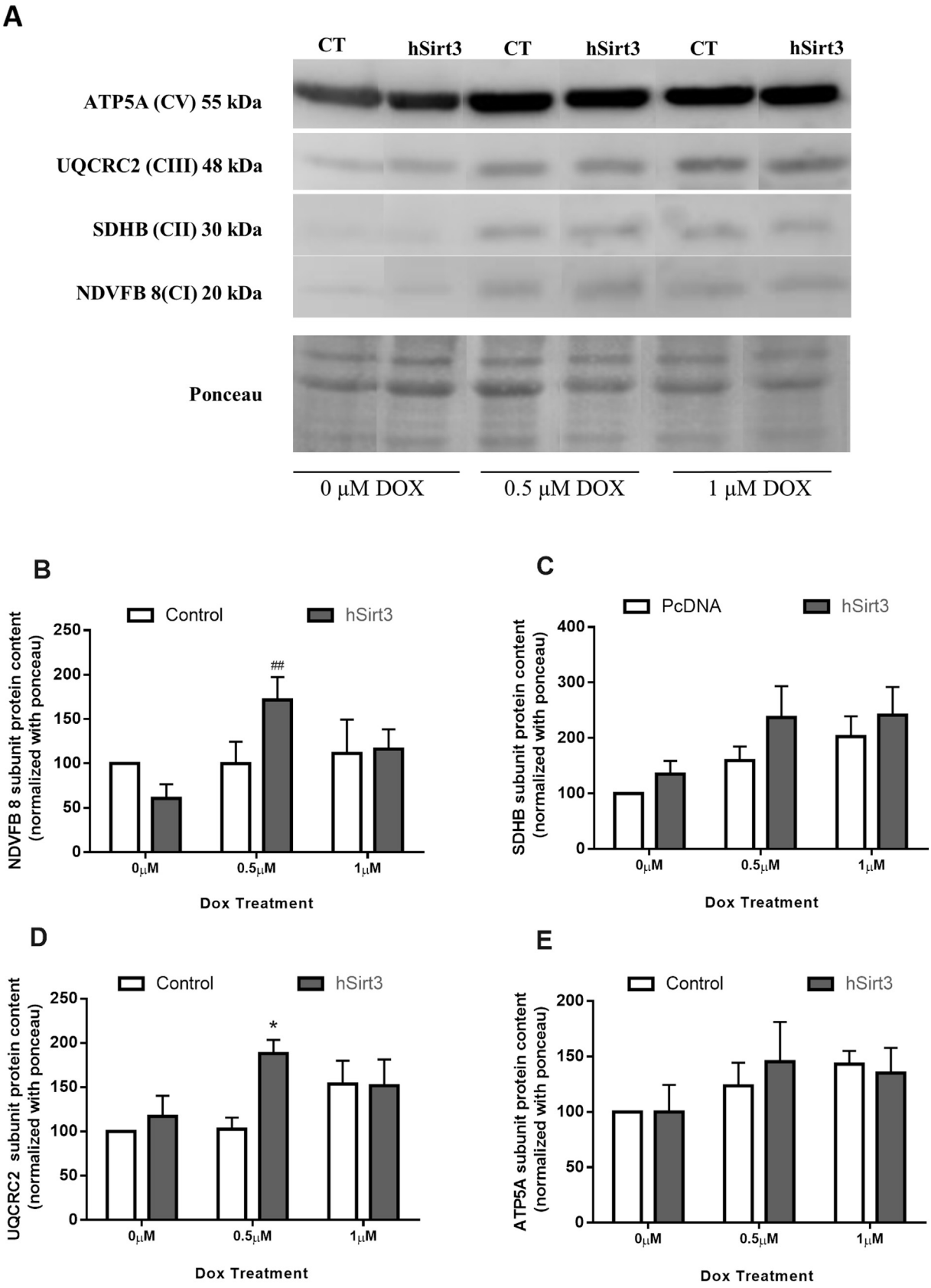

Fig. 3. Impact of modulation of Sirt3 expression on DOX-induced alterations in OXPHOS subunits content in H9c2 cardiomyoblasts. H9c2 cardiomyoblasts were subjected to Sirt3 overexpression (hSirt3) and respective control condition, and incubated with DOX (0, 0.5 and 1 μM) for 24 h. A) Representative image of protein content by Western blot of OXPHOS subunits. The image was cut in order to remove unwanted groups. Protein quantification of B) NDUFB8-CI (20 kDa), C) SDHB-CII (30 kDa), D) UQCRC2-CIII (47 kDa) and E) ATP5A-CV (53 kDa) by Western blot. Results were compared to the control in the absence of DOX and normalized to Ponceau staining. Data represents mean ± SEM of 3–4 independent experiments. One symbol = $p < 0.05$, two symbols = $p < 0.01$ and three symbols = $p < 0.001$. * vs control of the DOX concentration. # analysis in the same transfection condition.

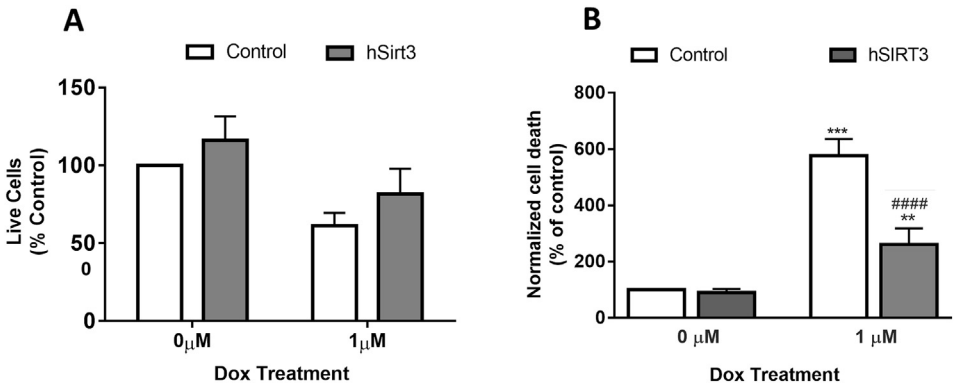

Fig. 4. Impact of modulation of Sirt3 expression on DOX-induced changes in H9c2 cell viability. To analyse the role of Sirt3 against DOX cardiotoxicity, H9c2 cardiomyoblasts were manipulated for Sirt3 overexpression (hSirt3) and respective control condition, and incubated with 1 μM DOX. A) Cell viability was analysed by flow cytometry upon labelling with Calcein-AM, to measure live cells, and Sytox Green, to quantify dead cells. Calcein-positive (live) cells and Sytox positive (dead) cells were measured in control conditions, containing only transfection reagent. B) Cell death was determined 24 h after 1 μM DOX treatment in H9c2 cells using the MultiTox-Glo multiplex cytotoxicity assay (Promega, Madison, WI), according to the manufacturer's instruction, and normalized with the SRB results (Cell death (%)/Cell mass (%) ratio). Results were normalized to the control without DOX. Data represents mean ± SEM of 3–5 independent experiments. One symbol = $p < 0.05$, two symbols = $p < 0.01$ and three symbols = $p < 0.001$. * vs control of the DOX concentration. # Analysis in the same transfection condition in all conditions of Fig. 4.

cathepsin D activities [41]. Thus, we analysed the ability of BER to induce cathepsin B or D activation on DOX-treated H9c2 cells (Fig. 10F–H). In the presence of 1 μM DOX the activity of cathepsin B was significantly increased (Fig. 10G), whereas BER *per se* had no effect on cathepsin B and D activities in H9c2 cells (Figs. 10G and 10H). Interestingly, the ratio between cathepsin D/cathepsin B increased in cells pre-treated with 10 μM BER and exposed 20 μM DOX (Fig. 10F), apparently due to a higher decrease in cathepsin B in these cells that did not reach statistical significance *per se* (Fig. 10G).

3.6. Modulation of mitophagy in DOX-treated cells by BER

All the data so far confirmed that DOX causes mitochondrial damage in H9c2 cardiomyoblasts, while BER increases Sirt3 and affords cardioprotection. It is known that the autophagic process is directed to eliminate damaged and dysfunctional mitochondria, a process known by mitophagy that may be triggered by the loss of $\Delta\Psi_m$ [55]. To evaluate if BER modulates mitophagy, we measured mitochondria and lysosome co-localization using Lysotracker Green and $TMRM^+$ (Fig. 11). We observed that untreated H9c2 cells presented normal cell morphology with a well-defined and filamentous mitochondrial network, as well as the presence of a small number of lysosomes, with little or no co-localization with mitochondria. BER did not appear to induce alterations in cell morphology. In fact, BER-treated H9c2 cells maintained the well-defined mitochondrial network with minimal lysosome-polarized mitochondria co-localization (Fig. 11). As expected DOX treatments induced changes in H9c2 cell morphology. H9c2 cells that were treated with low-DOX concentration contained a more fragmented mitochondrial network and a significant increase of lysosomes. The increased lysosomal accumulation co-localized with polarized mitochondria possibly leading to their degradation through a mitophagic process (Fig. 11). High-DOX treated H9c2 cells presented a more fragmented mitochondrial network and an extensive accumulation of acidic vesicles. Despite that fact, we observed that lysosome-polarized mitochondria co-localization was present, but in a much less extent than in low-DOX concentrations (Fig. 11). BER pre-treatment appeared to exert different effects in the presence of low and high DOX concentrations. We observed that BER pre-treatment before the administration of 1 μM DOX led to a decrease on lysosomal-polarized mitochondria co-localization. The opposite scenario happened with 20 μM DOX-treated cells. BER pre-treatment before incubation with the high-DOX concentration appeared to increase the co-localization between polarized mitochondria and acidic vesicles, suggesting that BER pre-treatment prevents mitophagy in cells treated with low-DOX concentrations, but likely promotes the elimination of mitochondria in the presence of the high-DOX concentrations. Still, it must be stressed that our experimental protocol is measuring the initial stages of mitochondrial lysosomal interaction and not later stages of mitophagy, in which mitochondria are degraded through that phenomenon.

3.7. Berberine induces mitochondrial biogenesis in DOX-treated cells

Changes in mitophagy may be accompanied by changes in mitochondrial biogenesis, to increase mitochondrial mass. It has been described that BER increases mitochondrial biogenesis mechanisms in skeletal muscle cells resulting in an improvement of mitochondrial function, associated with Sirt1 activation [35]. To determine whether mitochondrial biogenesis was also elicited by BER pre-treatment in DOX-exposed H9c2 cells, we measured TOM20 and Tfam protein content in our experimental conditions (Fig. 11). BER pre-treatment by itself did not alter TOM20 content (Fig. 12A, C). However, pre-treatment with BER before DOX treatment induced an increase in TOM20 content, when compared with untreated cells and with the respective DOX control. In respect to Tfam protein content (Fig. 12B, D), either BER or DOX alone did not alter Tfam content. However, when H9c2 cells were pre-treated with BER before DOX treatment, Tfam content significantly increased in comparison with the respective DOX concentration alone. This result suggests that BER pre-treatment induces mitochondrial biogenesis in the presence of DOX, possibly to compensate DOX-induced mitochondrial dysfunction.

4. Discussion

Doxorubicin is one of the most potent anticancer agents used against a wide range of tumours [1,4,56]. However, the cardiotoxicity associated with DOX-therapy has compromised its clinical application [57]. It has been proposed that the cardiotoxicity induced by DOX has a strong mitochondrial component with possible different mechanisms being involved, such as cell death and disruption of mitochondrial homeostasis, being oxidative stress one important component for DOX-induced cardiotoxicity [6,58]. The hypothesis of the present work is that BER may prevent DOX-induced cardiotoxicity, by increasing Sirt3 protein content.

DOX cardiotoxicity is especially relevant for adult survivors of paediatric malignancies. In a juvenile mouse model treated with DOX, the development of an abnormal vasculature resulted in higher susceptibility to myocardial infarction. Also, a decreased number of CPCs was observed after DOX treatment, suggesting that these undifferentiated cells are more susceptible to DOX, thus limiting the resistance of the treated heart to oxidative stress [9,59]. According to this, Angelis *et al.* reported also that adult and neonatal rat cardiomyocytes have different susceptibilities to DOX exposure, with the apoptotic pathway being more active in immature cells [60]. These authors demonstrated also that cardiomyocytes respond differently to DOX depending on their differentiation state [60]; results which were further confirmed by us in a cardiomyoblast cell line [15]. In the

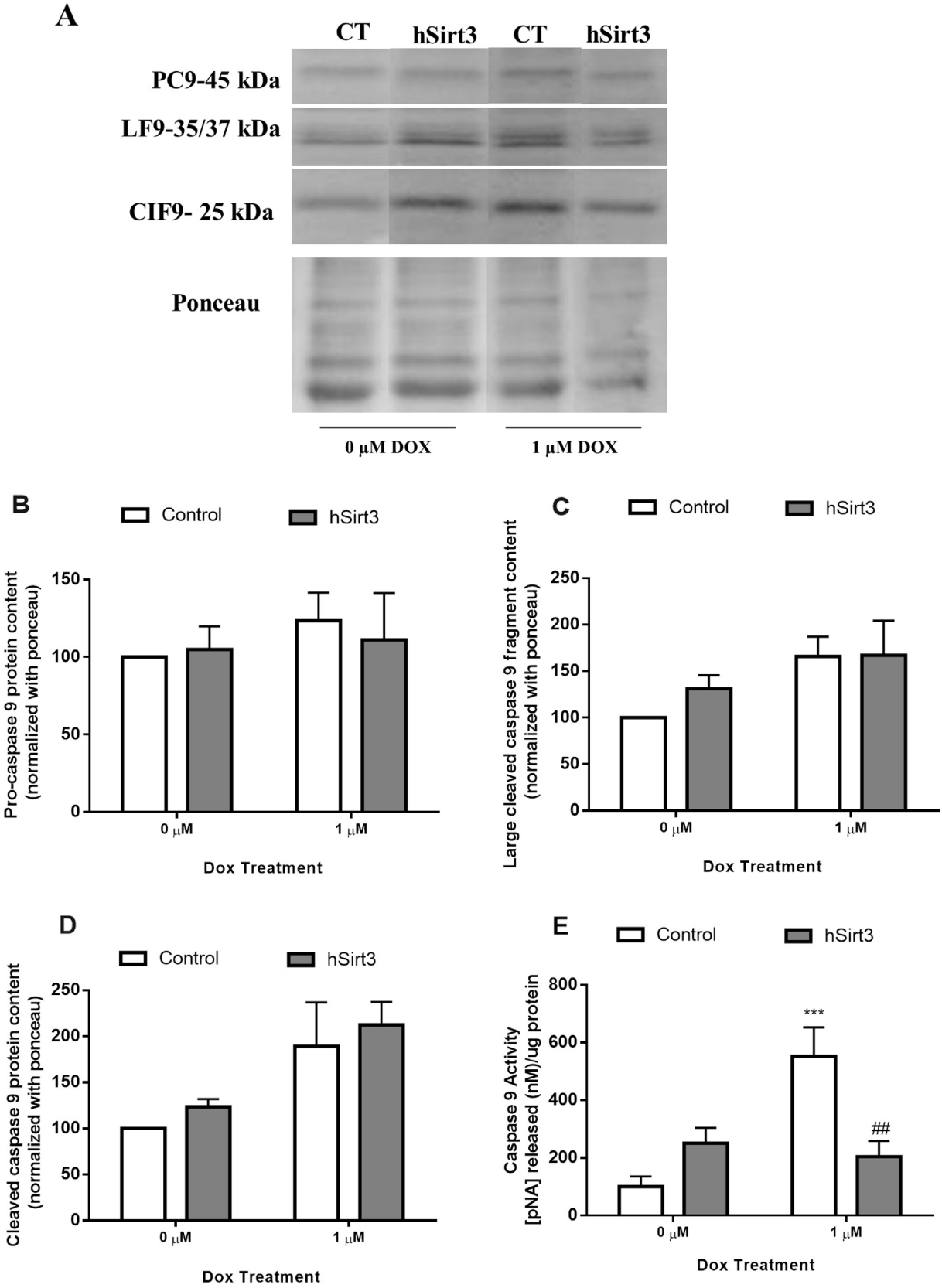

Fig. 5. Impact of the modulation of Sirt3 expression on DOX-induced changes in caspase-9 levels and activity in H9c2 cardiomyoblasts. H9c2 cardiomyoblasts were subjected to Sirt3 overexpression (hSirt3) and respective control conditions, and incubated with 1 μM DOX for 24 h. Protein content and fragmentation of caspase-9 was evaluated by Western blotting by analysing A) Representative image. The original blotting membrane was cut in order to remove unnecessary treatment groups. B) procaspase-9 (PC9) (45 kDa), C) large cleaved caspase-9 fragment (LF9) (35/37 kDa) and D) cleaved caspase-9 (ClF9) (25 kDa) bands. E) Caspase-9-like activity was also evaluated after Sirt3 overexpression, in the absence or presence of DOX. Data represents mean ± SEM of 3–4 independent experiments. Results were normalized to the control without DOX. One symbol = $p < 0.05$, two symbols = $p < 0.01$ and three symbols = $p < 0.001$. * vs control of the DOX concentration, # analysis in the same transfection condition throughout Fig. 5.

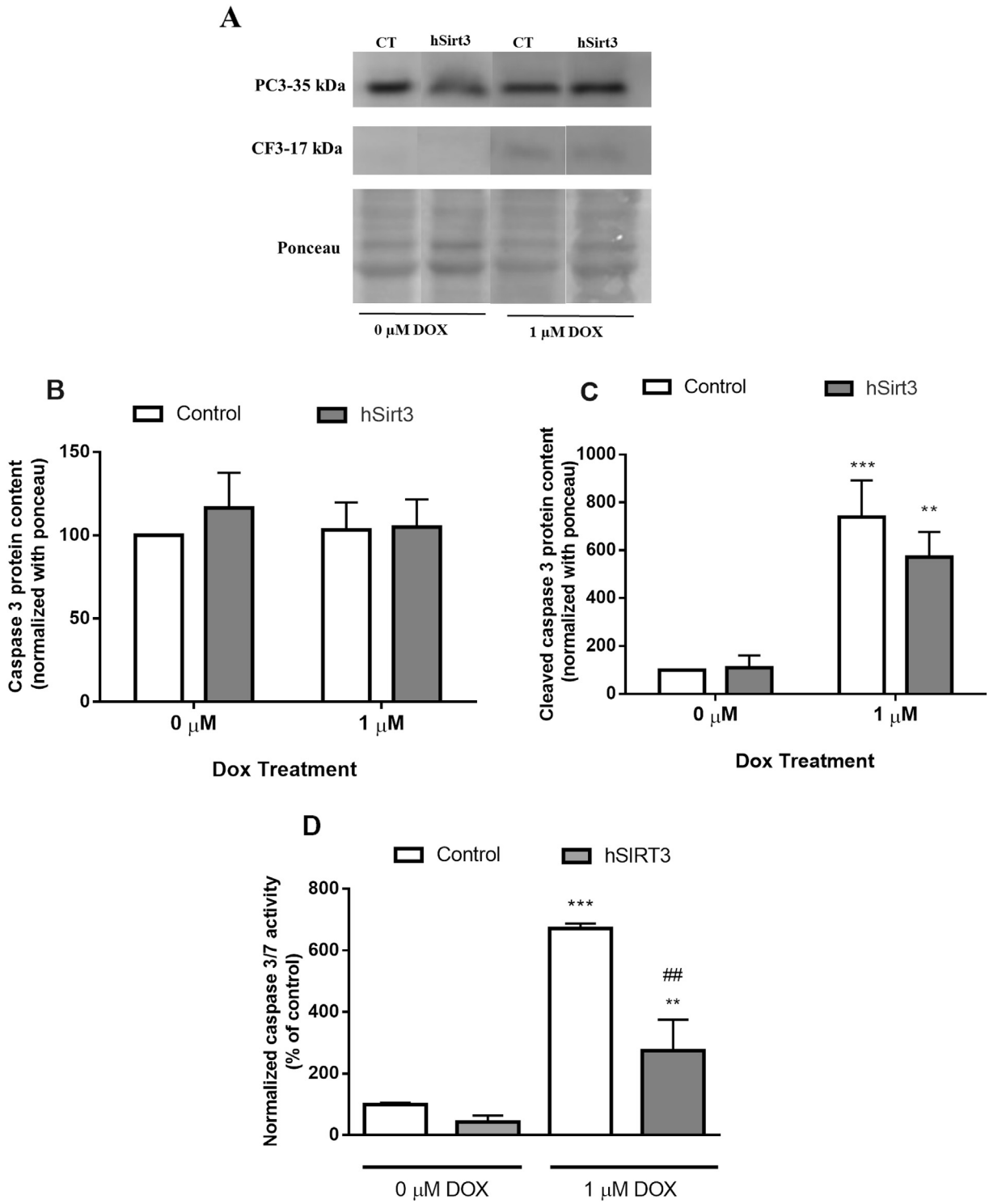

Fig. 6. Impact of the modulation of Sirt3 expression on DOX-induced changes in caspase-3 levels and activity in H9c2 cardiomyoblasts. H9c2 cardiomyoblasts were subjected to Sirt3 overexpression (hSirt3) and respective control condition, and incubated with1 μM Dox for 24 h. Protein content and fragmentation of caspase-3 was evaluated by Western blotting. A) Representative Western blot image. The original blotting membrane was cut in order to remove unnecessary treatment groups. B) procaspase-3 (PC3) (35 kDa) and C) cleaved caspase-3 fragment (CF 3) (17 kDa) bands. D) Caspase-3-like activity was also evaluated after Sirt3 overexpression. Results were normalized to the control cells in the absence of DOX. Data represents mean ± SEM of 3–4 independent experiments. One symbol = $p < 0.05$, two symbols = $p < 0.01$ and three symbols = $p < 0.001$. * vs control of the same concentration of DOX, # analysis in the same transfection condition.

present work, H9c2 cardiomyoblasts were used as a model for CPCs, since these cells have the ability to differentiate into adult skeletal muscle and cardiac cells [61]. We used DOX concentrations equivalent to those achieved in plasma after administration of therapeutic doses of DOX (0.5 and 1 μM), also adding a supra-physiological dosage (20 μM) to mimic a single acute treatment [14].

Considering that DOX inhibits Sirt3 expression [17,18], we first wondered whether Sirt3 regulation could prevent the toxic effects of DOX on H9c2 cardiomyoblasts. To answer this question, we investigated the impact of modulation of Sirt3 expression levels on DOX-

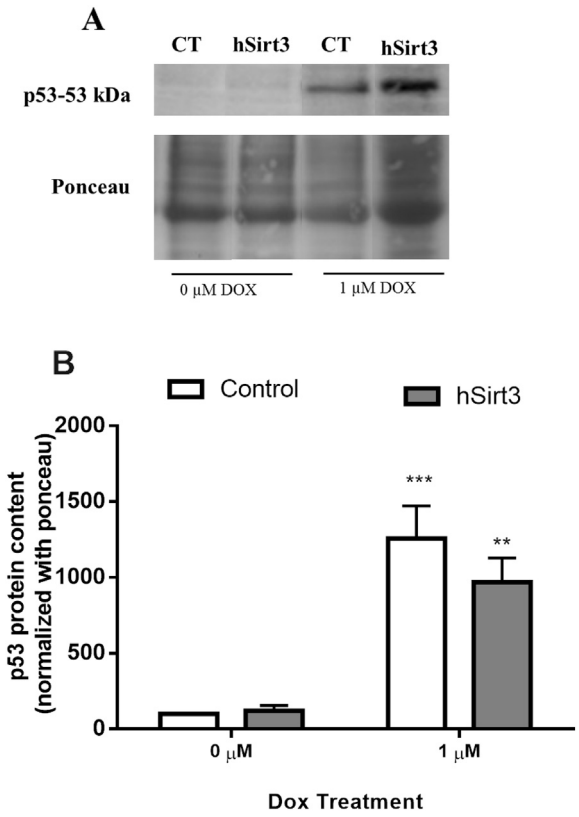

Fig. 7. Impact of the modulation of Sirt3 expression on DOX-induced changes in p53 levels in H9c2 cardiomyoblasts. H9c2 cardiomyoblasts were subjected to Sirt3 overexpression (hSirt3) and incubated with DOX (0, 0.5 and 1 μM) for 24 h. Protein content of p53 (53 kDa) was evaluated by Western blotting. A) Representative image of protein content. The original blotting membrane was cut to remove unnecessary treatment groups. B) Quantification of p53 expression. Results are normalized to the control transfected cells, in the absence of DOX. Data represents mean ± SEM of 3–4 independent experiments. One symbol = $p < 0.05$, two symbols = $p < 0.01$ and three symbols = $p < 0.001$. * vs control of the same concentration of DOX, # analysis in the same transfection condition.

induced cardiotoxicity on the H9c2 cell line. We observed that H9c2 cells overexpressed with a human Sirt3-flag construct (hSirt3) showed a higher expression of Sirt3 (Fig. S1). We next confirmed the cytotoxicity induced by DOX on the H9c2 cell line, observed as a decrease in cell mass (Fig. S3) and live cells for DOX treatment (Fig. 4), as well as by the increase of caspase 3 and 9 protein content and activities (Figs. 5 and 6), in accordance with previously described studies [13,50,62,63]. Nevertheless, mitochondrial depolarization and mitochondrial network fragmentation induced by low-DOX concentrations was also observed by using $TMRM^+$ as a mitochondrial-membrane potential-dependent fluorescent dye (Fig. 1). These results are according with our previous works [14,50], as well as with other studies showing a decrease in mitochondrial membrane potential after DOX treatment [64,65]. Importantly, we observed that the overexpression of Sirt3 prevented mitochondrial fragmentation induced by DOX, as observed by the cellular mitochondrial distribution and transmembrane electrical potential, indirectly measured as cell TMRM fluorescence (Fig. 1). These results agree with the fact that the overexpression of Sirt3 preserves mitochondrial network distribution and inhibition of DOX-induced cardiomyocyte death through the activation of the fusion protein optic atrophy 1 (OPA1) [19]. Sirt3 activity preserved the normal tubular shape of mitochondria during DOX-induced cytotoxicity on cardiomyocytes [19]. By comparing wild-type (WT) and mutant Sirt3 effects on HeLa cells, only WT Sirt3 was able to preserve mitochondrial morphology [19], which is also consistent with our results (Fig. 1).

Considering that DOX induces cell death in part by increasing oxidative stress, and that Sirt3 contributes to cell survival protecting mitochondria against oxidative stress [21,66], we investigated whether DOX influences Sirt3 expression influenced DOX-induced ROS production. Several reports considered that Sirt3 also prevented mitochondrial disruption caused by oxidative stress by deacetylating SOD2 [23,25], one of the main anti-oxidant enzymes shown to be decreased in cardiomyocytes after DOX treatment [64,65,67]. In our results, an increase of superoxide anion (Fig. 2) and SOD2 protein content (Fig. 9) was found in H9c2 cells treated with DOX, in agreement with Tokudome and collaborators when using neonatal cardiomyocytes [68]. Our results also showed that although Sirt3 overexpression decreased the detectable amount of superoxide anion and SOD2 protein content, but more visible on cells treated with BER. Sirt3 deacetylates and activates SOD2 [69] and its protective effect against ROS was better visible with acetyl versus total SOD2 protein content ratio. From these results, we can conclude that Sirt3 may have a contribution to reduce the oxidative stress induced by DOX including an indirect activation of other ROS-detoxifying enzymes, especially upon BER treatment. Moreover, Sirt3 deacetylates and activates the TCA cycle enzyme isocitrate dehydrogenase 2 (IDH2) and glutamate dehydrogenase in murine liver [21,70], both of which produce NADH in mitochondria. NADH in turn is required for glutathione reductase to convert oxidized into reduced glutathione, which is a crucial cofactor for mitochondrial glutathione peroxidase to scavenge oxidized species [69]. Another possibility that should be considered is the fact that Sirt3 deacetylates numerous components of the electron transport chain, being possible that this effect may reduce the production of superoxide anion caused by DOX by improving the efficacy of electron transport however nothing has been reported about this possible mechanism so far. We demonstrated in this work that DOX, non-treated H9c2 cells over-expressing Sirt3, promoted an increase of NADH dehydrogenase and succinate dehydrogenase subunits content (Fig. 3). Similar studies with the same type of end-points often yielded mixed results. Some studies reported that complex I and II activities were decreased after DOX treatment in heart mouse homogenates and H9c2 cells, although the protein content of these complexes was not decreased [71], while other studies also reported an increase of complex II protein content in heart lysates [72]. These differences probably occurred due to different experimental conditions used in each study, being possible that the increase of protein content of the respiratory complexes observed in our study may be due to a compensatory mechanism in order to revert the loss of activity observed after DOX treatment, although we did not measure that in our work. On the other hand, we found that the overexpression of Sirt3 increased the content of complex subunits after treatment with 0.5 μM DOX but not with 1 μM DOX (Fig. 3). These results strongly suggest, and contrarily to what was reported previously, that different concentrations of DOX can distinctively affect the role of Sirt3 within the cell, which is in agreement with the fact that Sirt3 deacetylates several components of the electron transport chain [38,73,74].

Nonetheless, other mechanisms may also be involved in the protective effect of Sirt3 modulation in preventing DOX-induced cardiotoxicity. Our results showed that although the overexpression of Sirt3 did not prevent the decrease in cell mass induced by DOX (Fig. 4), the overexpression of Sirt3 decreased the activity of caspases 3 and 9, and the amount of p53 protein (Figs. 5, 6 and 7), three parameters previously described by us as involved in cell death mechanisms induced by DOX [13,14]. So, it is also possible that the modulation of Sirt3 on p53 could prevent the toxicity induced by DOX. In fact, it is known that DOX promotes over-expression and activation of p53, Bax over-expression and induces its translocation to mitochondria [14], and that the activation of p53 may in turn induce alteration of mitochondrial membrane potential, leading to cytochrome *c* release, culminating with apoptosis [75,76]. Since Sirt3 inhibits p53 activation by promoting its deacetylation [76], and also Bax translocation to mitochondria by promoting ku70 protein interaction under stress conditions [66], it is also possible that Sirt3 can prevent DOX-induced apoptosis. Taken

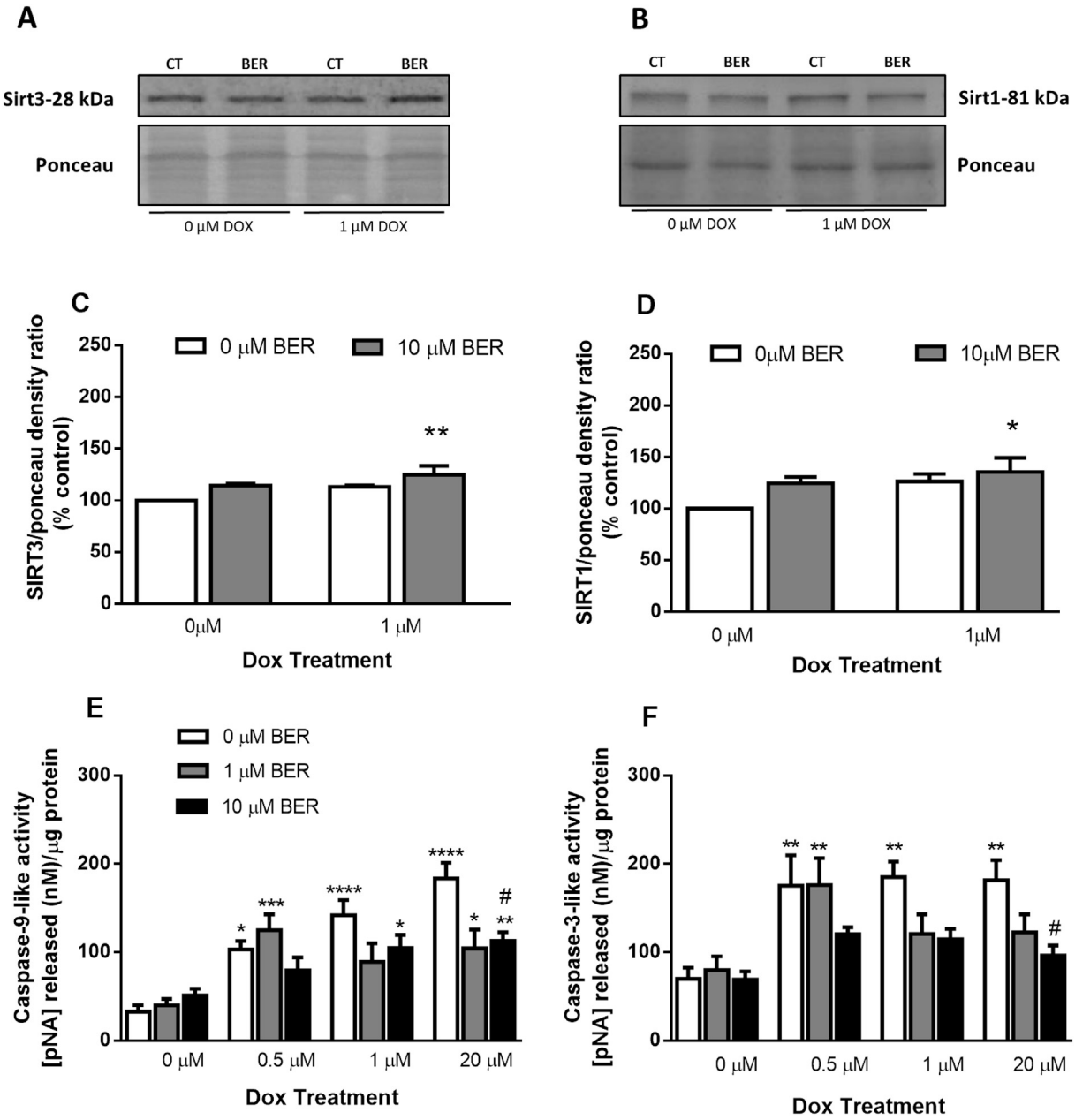

Fig. 8. Modulation of Sirtuin protein content by Berberine in DOX-treated H9c2 cardiomyoblasts is associated with prevention of DOX-induced caspase activation. H9c2 cells were treated with 1 or 10 μM berberine (BER) for 72 h and exposed to 0, 0.5, 1 or 20 μM DOX in the last 24 h. A–C) Sirt3 and B–D) Sirt1 protein content were evaluated by Western blotting. Data were represented in mean ± SEM of 4 independent experiments. The measurements of E) caspase-9 and F) caspase-3 like- activities were performed by colorimetric assays. Data were represented in mean ± SEM of 6 independent experiments. One symbol = $p < 0.05$, two symbols = $p < 0.01$ and three symbols = $p < 0.001$, four symbols = $p < 0.0001$ * vs control without BER and DOX treatment, # control of the same concentration of DOX.

together, Sirt3 modulation may confer protection against DOX-induced cardiotoxicity, probably by reducing the oxidative stress mechanisms and intrinsic cell death pathways, highlighting the pharmacological activation of Sirt3 as a promising approach to prevent the cardiotoxicity promoted by this anticancer agent. An example of Sirt3 activating molecules is BER, which was previously shown to activate Sirt3 [36]. Although nothing is currently known about the role of Sirt3-activation pathway on cardio-protection mechanisms induced by BER against DOX-induced cardiotoxicity, the cardio-protective effects of BER against the toxicity induced by DOX were already described [34,77–79]. Our present results showed that BER combined with DOX increase the expression of Sirt3 and Sirt1, although with a more prominent effect on Sirt3 (Fig. 8), indicating that BER can promote the activation of Sirt3 pathway in cardiomyocytes treated with DOX, a result which has never been described before. Considering that the modulation of Sirt3 promotes the inhibition of intrinsic apoptotic cell death pathways induced by DOX, we next questioned whether BER can prevent DOX-induced cardiotoxicity, and if confirmed what would be the mechanisms involved in BER protection against DOX toxicity. Our results showed that BER prevented DOX cytotoxicity on H9c2 cells induced by 1 and 20 μM DOX (Fig. S3), also preventing the activation of caspases − 9 and − 3 (Fig. 8). This decrease in caspase 9 and 3- like activities is in concordance with previous results [79].

Considering that the autophagy process plays an important role in the development of DOX-induced cardiomyopathy [80,81], and that Sirt3 pathway regulates autophagy [82], we next investigated if BER modulated autophagy upon DOX-induced toxicity. Our results showed that DOX, at lower concentrations (1 μM) promoted an increase of

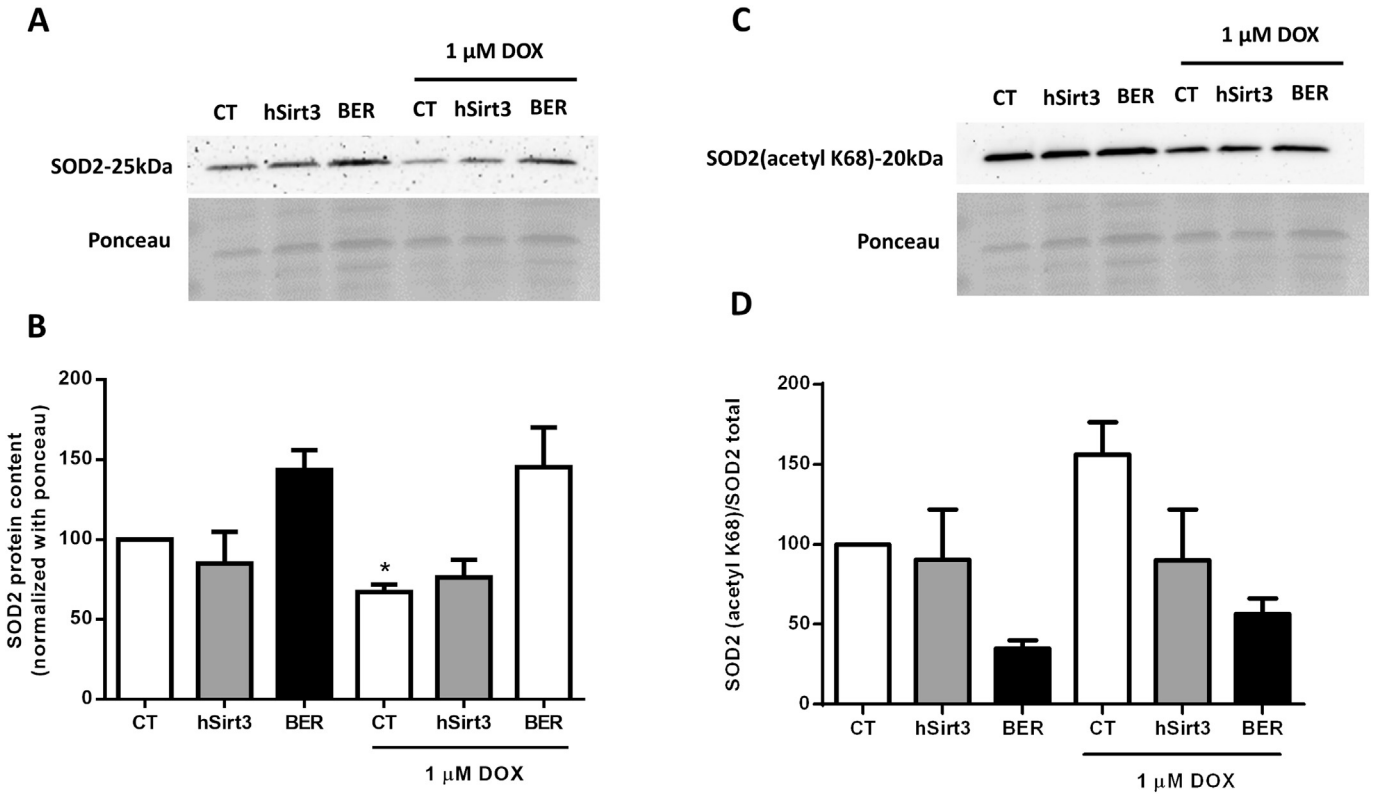

Fig. 9. Effects of Sirt3 overexpression and BER treatment on DOX-induced changes in SOD2 (total and acetylated) levels in H9c2 cardiomyoblasts. H9c2 cardiomyoblasts were subjected to Sirt3 overexpression (hSirt3) for 24 h or treated with 10 μM BER for 72 h and exposed to 1 μM DOX in the last 24 h. A–B) Total and C) acetylated SOD2 protein contents were evaluated by Western blotting. Results are normalized to control-transfected cells, in the absence of DOX. Data represents mean ± SEM of 3–4 independent experiments. $*p < 0.05$ vs control.

cathepsin B activity (Fig. 10), accompanied by a lysosome-mitochondrial co-localization (Fig. 11), which suggested mitophagy induction. At higher concentrations, DOX induced a more fragmented mitochondrial network and an extensive accumulation of acidic vesicles accompanied also by co-localization of lysosome with polarized mitochondria (Fig. 11). These results are in accordance with a previous study that showed a dual role of DOX in the autophagy process [51], showing that DOX induces autophagy at lower concentrations, while inhibiting the autophagy process at higher concentrations [51]. However, pre-treatment with BER may apparently block autophagy as observed by p62 and autophagosome accumulation (Fig. 11), since low p62 turnover and autophagosome accumulation may lead to autophagy impairment and consequent inability to degrade cargo [83]. This inability can result from the blockage of fusion between the autophagosome and the lysosome. We observed cathepsin B inhibition with BER pre-treatment in H9c2 cells treated with 1 μM DOX without a significant increase of cathepsin D activity (Fig. 10) that may result in lysosomal integrity preservation. These results also confirmed the blockage of autophagy process by BER, since lysosomal viability can be indirectly measured by cathepsin activity data and it is related to high cathepsin B and low cathepsin D activities [42]. Additionally, the decrease of co-localization between polarized mitochondria and lysosomes promoted by BER in DOX-treated cells suggested that BER may apparently block mitophagy for lower-DOX treatments. However, this data must be interpreted carefully. In fact, it is known that Lysotracker Green only stains acid vesicles and as described $TMRM^+$ only accumulates on polarized mitochondria. Mitophagy is normally triggered by loss of $\Delta\Psi m$ and after cargo degradation, lysosome vesicles lose their acidic pH. Then our data may only show initial stages of mitophagy. However, more experiments need to be done in order to fully understand which role BER plays in the elimination of DOX-induced damaged mitochondria.

The effect of BER with higher concentrations of DOX on autophagy markers is different. Although, an accumulation of p62 protein was observed, a relevant conversion of LC3-I into LC3-II was also detected (Fig. 10), which may be indicative of autophagosome formation [84], accompanied by a reduction in the accumulation of acidic vesicles. These observations may suggest that BER promotes the activation of a protective autophagy mechanism in order to eliminate damaged protein that accumulates in cells [85]. On the other hand, cathepsin B inhibition led to a massive increase of cathepsin D/cathepsin B ratio. This may indicate that BER modulates lysosomal cathepsin B in order to degrade the cargo targeted for elimination despite the possible inability of autophagosome/lysosome fusion. Moreover, lysosomal integrity may possibly be decreased due to accumulation of cathepsin D that may damage the lysosomal membrane and culminate with the lysosomal-related cell death [86]. Lysosomal- related cell death may be caspase-independent and can possibly justify the modest protection afforded by BER [86]. Thus, it is possible that BER may have the capacity to modulate the dual effect of DOX on the autophagy process, reducing autophagy at lower concentrations, and also promoting autophagy, which is blocked by DOX at higher concentrations. In fact, it has also been described that BER exerts a cardioprotective effect by promoting the induction of autophagy through the inhibition of Mammalian Target of Rapamycin (mTOR), p38 and ERK1/2 MAPK signalling pathways [87], while it has also the capacity to reduce the excessive autophagy in cardiomyocytes [88].

Another mechanism that may also explain the cardioprotective effect of BER is the induction of mitochondrial biogenesis, suggested by the increase of the mitochondrial outer membrane marker TOM20 (Fig. 12) after pre-treatment with BER, a possible indication of increased mitochondrial mass. Still, one has to consider that the increase of mitochondrial mass may be influenced by the accumulation of damaged mitochondria that cannot be eliminated by mitophagy. Considering that BER modulation of Sirt1 activates mechanisms of mitochondrial biogenesis in skeletal muscle cells [35], and that the modulation of Sirt3 may also in turn promote the induction of

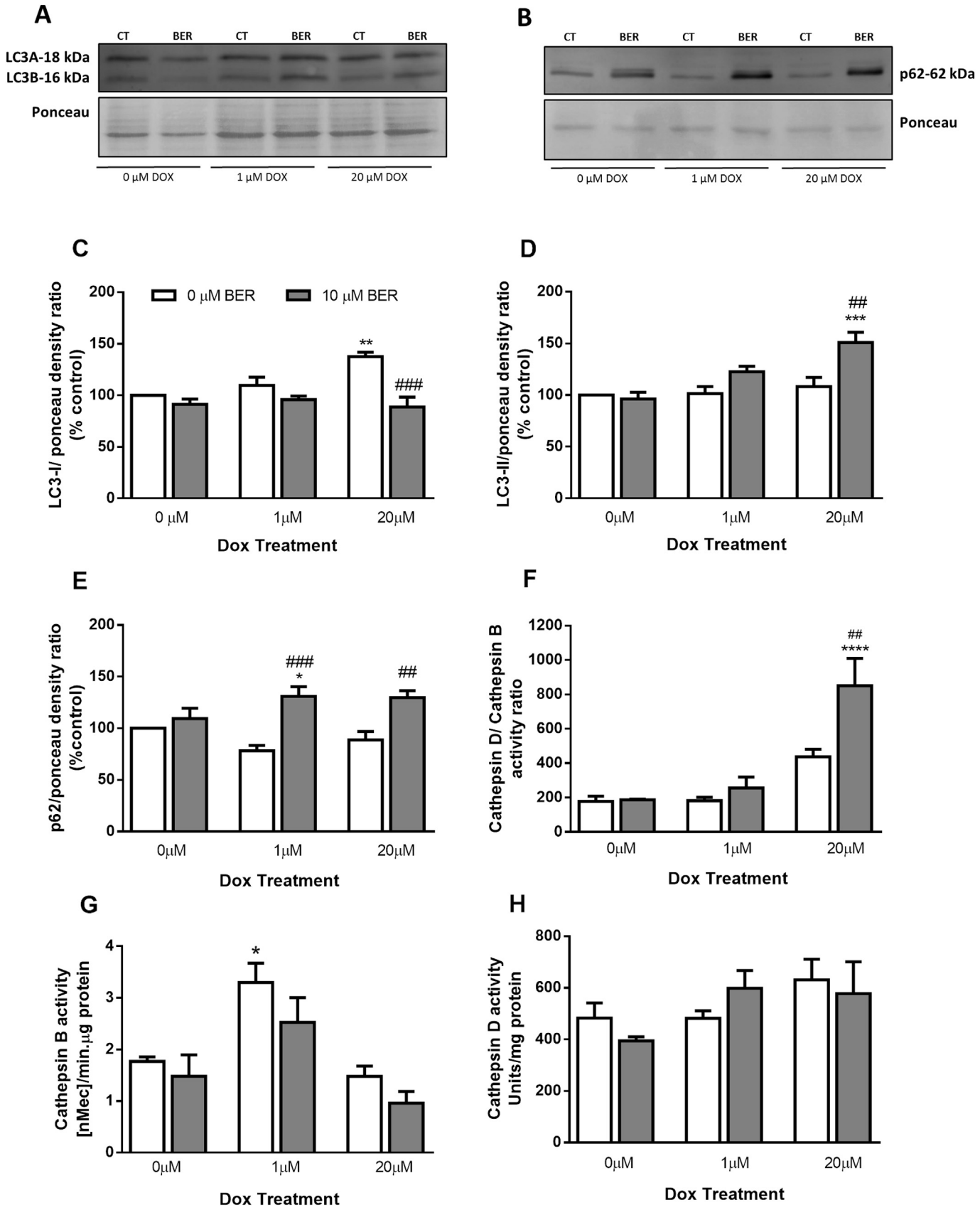

Fig. 10. Modulation of DOX-induced autophagy by berberine in H9c2 cardiomyoblasts. H9c2 cells were treated with 10 μM berberine (BER) for 72 h and exposed to 0, 1 or 20 μM DOX in the last 24 h. A,C,D) LC3-I/II and B,E) P62 protein contents were evaluated by Western blotting. Data were represented in mean ± SEM of 5 independent experiments. F–H) Activities of cathepsins D and B were measured by spectrophotometric and fluorimetric assays, respectively. Data were represented in mean ± SEM of 5 independent experiments. One symbol = $p < 0.05$, two symbols = $p < 0.01$ and three symbols = $p < 0.001$, four symbols = $p < 0.0001$ * vs control without BER and DOX treatment, # control of the same concentration of DOX.

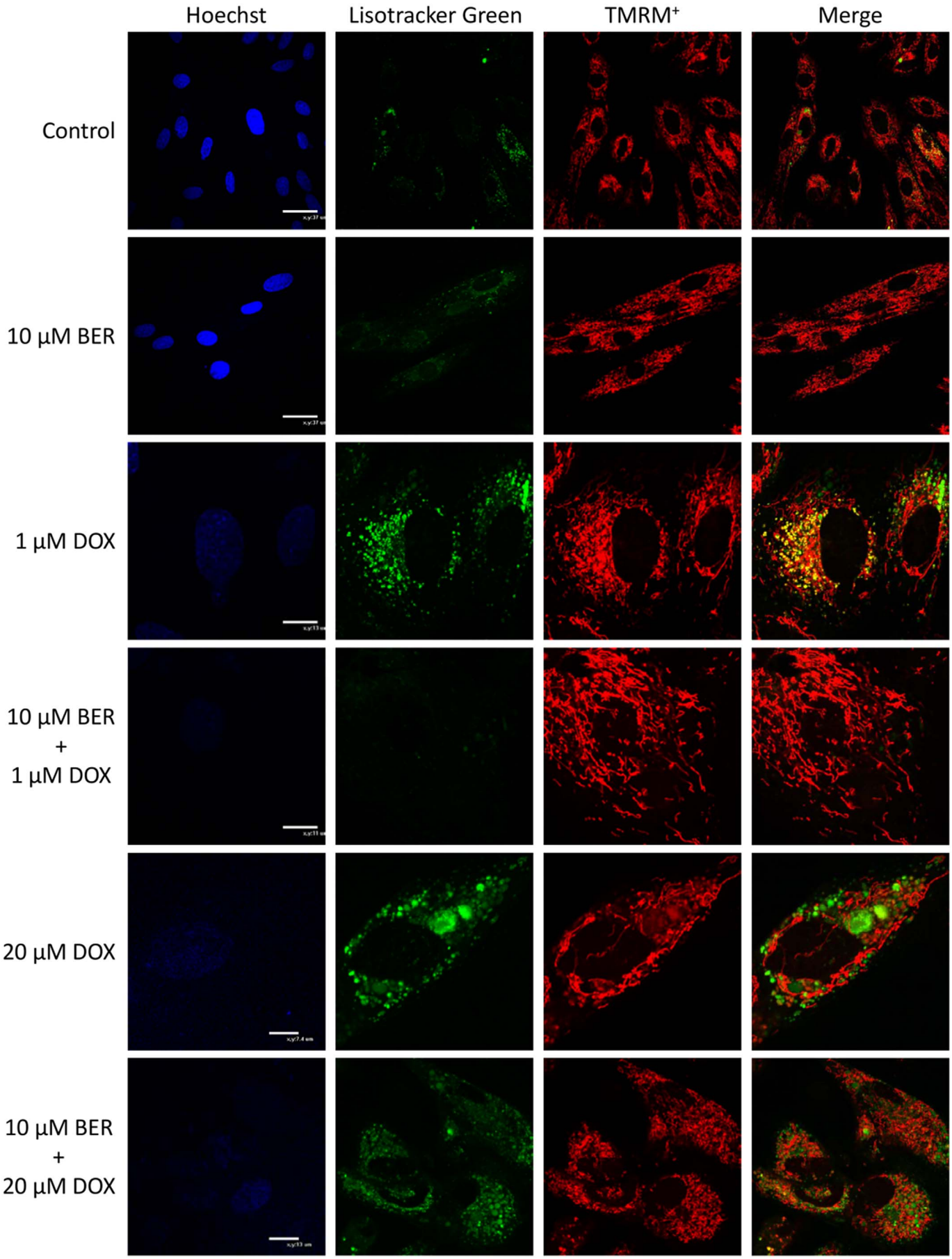

(caption on next page)

Fig. 11. Lysosomes and polarized mitochondria co-localization in H9c2 cells treated with in BER and or DOX. H9c2 cells were treated with 10 μM BER for 72 h and exposed to 0, 1 or 20 μM DOX in the last 24 h. Live cells were then stained with Lysotracker green to label lysosomes, $TMRM^+$ to label polarized mitochondria, and Hoechst 33342 to label nuclei. Images show different magnifications to allow a better identification of DOX effects.

mitochondrial biogenesis, it is also possible that the modulation of both Sirt1 and Sirt3 by BER may also be responsible by the cardioprotective effects of this compound. In agreement, our results showed that BER pre-treatment of H9c2 cells resulted in Sirt1, Sirt3 (Fig. 8) and Tfam (Fig. 12) upregulation in DOX-treated groups. Thus, it is possible that Sirt1 and Sirt3 may be involved in increased mitochondrial biogenesis in BER-treated H9c2 cells, probably through the downstream activation of Peroxisome proliferator-activated receptor gamma co-activator 1-alpha (PGC-1) and Tfam. In fact, it is known that Tfam once activated induces the transcription and the replication of mtDNA which translates in more functional mitochondria [89,90]. Additionally, Sirt3 can be regulated by PGC-1 activation and it may lead to the upregulation of ROS-detoxifying mechanisms, by stimulating the *de novo* formation of respiratory chain components [91]. Moreover, it is also possible that BER can upregulate Sirt3 expression in both DOX treatments, representing thus another protective mechanism against DOX-induced oxidative damage.

5. Conclusion

Every year the incidence of cancer is increasing worldwide. Once DOX is one of the most widely used and efficient drug in cancer treatment, there is a pressing need to decrease the adverse effects of DOX, finding therapeutic strategies to inhibit cardiotoxicity. In our study, we observed that BER pre-conditioning afforded protection against DOX-induced cardiotoxicity by inhibiting caspase-dependent mitochondrial apoptosis pathway, promoting the regulation of autophagy and by inducing mitochondrial biogenesis, probably through the modulation of Sirt3-mediated pathways. The data obtained in this work must be confirmed in vivo using a dual model of cardiac cytotoxicity/chemotherapeutic efficacy in order to demonstrate that BER, when used with DOX decreases cardiotoxicity without compromising the anticancer efficacy. Regarding the latter, the fact that BER potentiates the anticancer effect of DOX in different types of cancer [30,92,93], strengthens BER and DOX co-administration as a promising approach to counteract DOX-induced cardiotoxicity in cancer treatment.

Supplementary data to this article can be found online at http://dx.doi.org/10.1016/j.bbadis.2017.07.030.

Transparency Document

The http://dx.doi.org/10.1016/j.bbadis.2017.07.030 associated with this article can be found, in online version.

Acknowledgements

We thank Dr. Michael Sack (MD, PhD) for providing us the hSIRT3 construct. This work was funded by FEDER funds through the Operational Programme Competitiveness Factors—COMPETE and national funds by FCT - Foundation for Science and Technology under research grants PTDC/DTP-FTO/1180/2012, PTDC/DTP-FTO/2433/2014, POCI-01-0145-FEDER-016659, and strategic project POCI-01-0145-FEDER-007440. Also supported by QREN project 4832 with reference CENTRO- 07-ST24-FEDER-002008 financed through FEDER. ARC (SFRH/BD/103399/2014) and CD (SFRH/BD/100341/2014) were supported by FCT PhD-fellowships and TC-O (SFRH/BPD/101169/2014) and TLS (SFRH/BPD/75959/2011) were supported by FCT Post-Doctoral fellowships. RAA was supported by Program of Competitive Growth of Kazan Federal University and subsidy allocated to Kazan Federal University for the state assignment in the sphere of scientific activities.

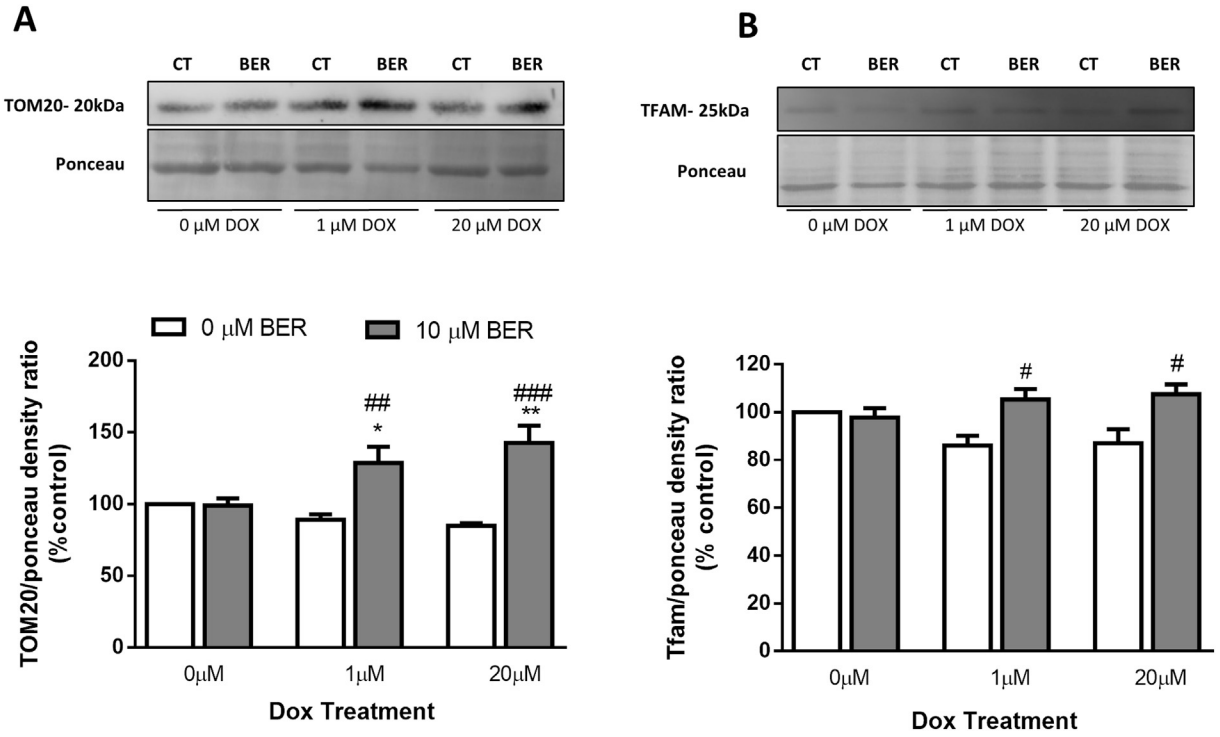

Fig. 12. BER induces mitochondrial biogenesis in DOX-treated H9c2 cardiomyoblasts. H9c2 cells were treated with 10 μM BER for 72 h and incubated with 0, 1 or 20 μM DOX in the last 24 h. A) TOM20 and B) TFAM protein contents were evaluated by Western blotting. Data were represented in mean ± SEM of 4 independent experiments. One symbol = $p < 0.05$, two symbols = $p < 0.01$ and three symbols = $p < 0.001$, four symbols = $p < 0.0001$ * vs control without BER and DOX treatment, # control of the same concentration of DOX.

Conflict of interest

The author(s) declare(s) that there are no conflicts of interest regarding the publication of this paper. The funding agencies had no role in the decision to publish.

References

[1] C. Carvalho, et al., Doxorubicin: the good, the bad and the ugly effect, Curr. Med. Chem. 16 (25) (2009) 3267–3285.
[2] G.C. Pereira, et al., Drug-induced cardiac mitochondrial toxicity and protection: from doxorubicin to carvedilol, Curr. Pharm. Des. 17 (20) (2011) 2113–2129.
[3] G. Bonadonna, et al., Clinical evaluation of adriamycin, a new antitumour antibiotic, Br. Med. J. 3 (5669) (1969) 503–506.
[4] R. Hrdina, et al., Anthracycline-induced cardiotoxicity, Acta Med. (Hradec Kralove) 43 (3) (2000) 75–82.
[5] E.A. Lefrak, et al., A clinicopathologic analysis of adriamycin cardiotoxicity, Cancer 32 (2) (1973) 302–314.
[6] F.S. Carvalho, et al., Doxorubicin-induced cardiotoxicity: from bioenergetic failure and cell death to cardiomyopathy, Med. Res. Rev. 34 (1) (2014) 106–135.
[7] C. Bearzi, et al., Human cardiac stem cells, Proc. Natl. Acad. Sci. U. S. A. 104 (35) (2007) 14068–14073.
[8] A.P. Beltrami, et al., Adult cardiac stem cells are multipotent and support myocardial regeneration, Cell 114 (6) (2003) 763–776.
[9] E. Piegari, et al., Doxorubicin induces senescence and impairs function of human cardiac progenitor cells, Basic Res. Cardiol. 108 (2) (2013) 334.
[10] D. Cesselli, et al., Effects of age and heart failure on human cardiac stem cell function, Am. J. Pathol. 179 (1) (2011) 349–366.
[11] C. Chimenti, et al., Senescence and death of primitive cells and myocytes lead to premature cardiac aging and heart failure, Circ. Res. 93 (7) (2003) 604–613.
[12] M. Rota, et al., Diabetes promotes cardiac stem cell aging and heart failure, which are prevented by deletion of the p66shc gene, Circ. Res. 99 (1) (2006) 42–52.
[13] V.A. Sardao, et al., Doxorubicin-induced mitochondrial dysfunction is secondary to nuclear p53 activation in H9c2 cardiomyoblasts, Cancer Chemother. Pharmacol. 64 (4) (2009) 811–827.
[14] V.A. Sardao, et al., Morphological alterations induced by doxorubicin on H9c2 myoblasts: nuclear, mitochondrial, and cytoskeletal targets, Cell Biol. Toxicol. 25 (3) (2009) 227–243.
[15] A.F. Branco, et al., Differentiation-dependent doxorubicin toxicity on H9c2 cardiomyoblasts, Cardiovasc. Toxicol. 12 (4) (2012) 326–340.
[16] A.C. Moreira, et al., Mitochondrial apoptosis-inducing factor is involved in doxorubicin-induced toxicity on H9c2 cardiomyoblasts, Biochim. Biophys. Acta 1842 (12 Pt A) (2014) 2468–2478.
[17] K.G. Cheung, et al., Sirtuin-3 (SIRT3) protein attenuates doxorubicin-induced oxidative stress and improves mitochondrial respiration in H9c2 cardiomyocytes, J. Biol. Chem. 290 (17) (2015) 10981–10993.
[18] I. Marques-Aleixo, et al., Physical exercise prior and during treatment reduces subchronic doxorubicin-induced mitochondrial toxicity and oxidative stress, Mitochondrion 20 (2015) 22–33.
[19] S.A. Samant, et al., SIRT3 deacetylates and activates OPA1 to regulate mitochondrial dynamics during stress, Mol. Cell. Biol. 34 (5) (2014) 807–819.
[20] M.N. Sack, T. Finkel, Mitochondrial metabolism, sirtuins, and aging, Cold Spring Harb. Perspect. Biol. 4 (12) (2012).
[21] D.B. Lombard, et al., Mammalian Sir2 homolog SIRT3 regulates global mitochondrial lysine acetylation, Mol. Cell. Biol. 27 (24) (2007) 8807–8814.
[22] E. Verdin, et al., Sirtuin regulation of mitochondria: energy production, apoptosis, and signaling, Trends Biochem. Sci. 35 (12) (2010) 669–675.
[23] X. Qiu, et al., Calorie restriction reduces oxidative stress by SIRT3-mediated SOD2 activation, Cell Metab. 12 (6) (2010) 662–667.
[24] S. Someya, T.A. Prolla, Mitochondrial oxidative damage and apoptosis in age-related hearing loss, Mech. Ageing Dev. 131 (7-8) (2010) 480–486.
[25] R. Tao, et al., Sirt3-mediated deacetylation of evolutionarily conserved lysine 122 regulates MnSOD activity in response to stress, Mol. Cell 40 (6) (2010) 893–904.
[26] C. Koentges, et al., SIRT3 deficiency impairs mitochondrial and contractile function in the heart, Basic Res. Cardiol. 110 (4) (2015) 36.
[27] S. Winnik, et al., Protective effects of sirtuins in cardiovascular diseases: from bench to bedside, Eur. Heart J. 36 (48) (2015) 3404–3412.
[28] S. Letasiova, et al., Antiproliferative activity of berberine in vitro and in vivo, Biomed. Pap. Med. Fac. Univ. Palacky Olomouc Czech Repub. 149 (2) (2005) 461–463.
[29] T.L. Serafim, et al., Different concentrations of berberine result in distinct cellular localization patterns and cell cycle effects in a melanoma cell line, Cancer Chemother. Pharmacol. 61 (6) (2008) 1007–1018.
[30] N. Tong, et al., Berberine sensitizes mutliple human cancer cells to the anticancer effects of doxorubicin in vitro, Oncol. Lett. 3 (6) (2012) 1263–1267.
[31] A. Shirwaikar, et al., In vitro antioxidant studies on the benzyl tetra isoquinoline alkaloid berberine, Biol. Pharm. Bull. 29 (9) (2006) 1906–1910.
[32] Y. Hong, et al., Effect of berberine on regression of pressure-overload induced cardiac hypertrophy in rats, Am. J. Chin. Med. 30 (4) (2002) 589–599.
[33] J.A. Marin-Neto, et al., Cardiovascular effects of berberine in patients with severe congestive heart failure, Clin. Cardiol. 11 (4) (1988) 253–260.
[34] C.W. Lau, et al., Cardiovascular actions of berberine, Cardiovasc. Drug Rev. 19 (3) (2001) 234–244.
[35] A.P. Gomes, et al., Berberine protects against high fat diet-induced dysfunction in muscle mitochondria by inducing SIRT1-dependent mitochondrial biogenesis, Biochim. Biophys. Acta 1822 (2) (2012) 185–195.
[36] J.S. Teodoro, et al., Berberine reverts hepatic mitochondrial dysfunction in high-fat fed rats: a possible role for SirT3 activation, Mitochondrion 13 (6) (2013) 637–646.
[37] Z. Lu, et al., SIRT3-dependent deacetylation exacerbates acetaminophen hepatotoxicity, EMBO Rep. 12 (8) (2011) 840–846.
[38] J. Bao, et al., Characterization of the murine SIRT3 mitochondrial localization sequence and comparison of mitochondrial enrichment and deacetylase activity of long and short SIRT3 isoforms, J. Cell. Biochem. 110 (1) (2010) 238–247.
[39] I. Romero-Calvo, et al., Reversible Ponceau staining as a loading control alternative to actin in Western blots, Anal. Biochem. 401 (2) (2010) 318–320.
[40] M.M. Bradford, A rapid and sensitive method for the quantitation of microgram quantities of protein utilizing the principle of protein-dye binding, Anal. Biochem. 72 (1976) 248–254.
[41] I. Vega-Naredo, A. Coto-Montes, Physiological autophagy in the Syrian hamster Harderian gland, Methods Enzymol. 452 (2009) 457–476.
[42] I. Vega-Naredo, et al., Sexual dimorphism of autophagy in Syrian hamster Harderian gland culminates in a holocrine secretion in female glands, Autophagy 5 (7) (2009) 1004–1017.
[43] T. Finkel, C.X. Deng, R. Mostoslavsky, Recent progress in the biology and physiology of sirtuins, Nature 460 (7255) (2009) 587–591.
[44] E. Pirinen, G. Lo Sasso, J. Auwerx, Mitochondrial sirtuins and metabolic homeostasis, Best Pract. Res. Clin. Endocrinol. Metab. 26 (6) (2012) 759–770.
[45] V. Gogvadze, S. Orrenius, B. Zhivotovsky, Mitochondria as targets for chemotherapy, Apoptosis 14 (4) (2009) 624–640.
[46] L.L. Chan, et al., Rapid image-based cytometry for comparison of fluorescent viability staining methods, J. Fluoresc. 22 (5) (2012) 1301–1311.
[47] Y. Octavia, et al., Doxorubicin-induced cardiomyopathy: from molecular mechanisms to therapeutic strategies, J. Mol. Cell. Cardiol. 52 (6) (2012) 1213–1225.
[48] M.H. Liu, et al., Resveratrol inhibits doxorubicin-induced cardiotoxicity via sirtuin 1 activation in H9c2 cardiomyocytes, Exp. Ther. Med. 12 (2) (2016) 1113–1118.
[49] P. Altieri, et al., Testosterone antagonizes doxorubicin-induced senescence of cardiomyocytes, J. Am. Heart Assoc. (2016) **5**(1).
[50] C.M. Deus, et al., Stimulating basal mitochondrial respiration decreases doxorubicin apoptotic signaling in H9c2 cardiomyoblasts, Toxicology 334 (2015) 1–11.
[51] Y.W. Zhang, et al., Cardiomyocyte death in doxorubicin-induced cardiotoxicity, Arch. Immunol. Ther. Exp. 57 (6) (2009) 435–445.
[52] B.J. Sishi, et al., Autophagy upregulation promotes survival and attenuates doxorubicin-induced cardiotoxicity, Biochem. Pharmacol. 85 (1) (2013) 124–134.
[53] S.K. Goswami, D.K. Das, Autophagy in the myocardium: dying for survival? Exp. Clin. Cardiol. 11 (3) (2006) 183–188.
[54] G. Bjorkoy, et al., Monitoring autophagic degradation of p62/SQSTM1, Methods Enzymol. 452 (2009) 181–197.
[55] D. Dutta, et al., Contribution of impaired mitochondrial autophagy to cardiac aging: mechanisms and therapeutic opportunities, Circ. Res. 110 (8) (2012) 1125–1138.
[56] K.B. Wallace, Doxorubicin-induced cardiac mitochondrionopathy, Pharmacol. Toxicol. 93 (3) (2003) 105–115.
[57] C. Zhang, et al., Resveratrol attenuates doxorubicin-induced cardiomyocyte apoptosis in mice through SIRT1-mediated deacetylation of p53, Cardiovasc. Res. 90 (3) (2011) 538–545.
[58] T. Simunek, et al., Anthracycline-induced cardiotoxicity: overview of studies examining the roles of oxidative stress and free cellular iron, Pharmacol. Rep. 61 (1) (2009) 154–171.
[59] C. Huang, et al., Juvenile exposure to anthracyclines impairs cardiac progenitor cell function and vascularization resulting in greater susceptibility to stress-induced myocardial injury in adult mice, Circulation 121 (5) (2010) 675–683.
[60] A. De Angelis, et al., Anthracycline cardiomyopathy is mediated by depletion of the cardiac stem cell pool and is rescued by restoration of progenitor cell function, Circulation 121 (2) (2010) 276–292.
[61] J. Hescheler, et al., Morphological, biochemical, and electrophysiological characterization of a clonal cell (H9c2) line from rat heart, Circ. Res. 69 (6) (1991) 1476–1486.
[62] A.J. Dirks-Naylor, et al., The effects of acute doxorubicin treatment on proteome lysine acetylation status and apical caspases in skeletal muscle of fasted animals, J. Cachex. Sarcopenia Muscle 4 (3) (2013) 239–243.
[63] L.A. Ahmed, S.A. El-Maraghy, Nicorandil ameliorates mitochondrial dysfunction in doxorubicin-induced heart failure in rats: possible mechanism of cardioprotection, Biochem. Pharmacol. 86 (9) (2013) 1301–1310.
[64] H.C. Lai, et al., Propofol ameliorates doxorubicin-induced oxidative stress and cellular apoptosis in rat cardiomyocytes, Toxicol. Appl. Pharmacol. 257 (3) (2011) 437–448.
[65] S. Su, et al., Sesamin ameliorates doxorubicin-induced cardiotoxicity: involvement of Sirt1 and Mn-SOD pathway, Toxicol. Lett. 224 (2) (2014) 257–263.
[66] N.R. Sundaresan, et al., SIRT3 is a stress-responsive deacetylase in cardiomyocytes that protects cells from stress-mediated cell death by deacetylation of Ku70, Mol. Cell. Biol. 28 (20) (2008) 6384–6401.
[67] H.J. Chae, et al., Radiation protects adriamycin-induced apoptosis, Immunopharmacol. Immunotoxicol. 27 (2) (2005) 211–232.
[68] T. Tokudome, et al., Ventricular nonmyocytes inhibit doxorubicin-induced myocyte apoptosis: involvement of endogenous endothelin-1 as a paracrine factor, Endocrinology 145 (5) (2004) 2458–2466.
[69] M. Tanno, et al., Emerging beneficial roles of sirtuins in heart failure, Basic Res. Cardiol. 107 (4) (2012) 273.
[70] C. Schlicker, et al., Substrates and regulation mechanisms for the human mitochondrial sirtuins Sirt3 and Sirt5, J. Mol. Biol. 382 (3) (2008) 790–801.

[71] Y. Zhao, et al., Redox proteomic identification of HNE-bound mitochondrial proteins in cardiac tissues reveals a systemic effect on energy metabolism after doxorubicin treatment, Free Radic. Biol. Med. 72 (2014) 55–65.
[72] S. Granados-Principal, et al., Hydroxytyrosol ameliorates oxidative stress and mitochondrial dysfunction in doxorubicin-induced cardiotoxicity in rats with breast cancer, Biochem. Pharmacol. 90 (1) (2014) 25–33.
[73] B.H. Ahn, et al., A role for the mitochondrial deacetylase Sirt3 in regulating energy homeostasis, Proc. Natl. Acad. Sci. U. S. A. 105 (38) (2008) 14447–14452.
[74] H. Cimen, et al., Regulation of succinate dehydrogenase activity by SIRT3 in mammalian mitochondria, Biochemistry 49 (2) (2010) 304–311.
[75] B. Calenic, et al., p53-Pathway activity and apoptosis in hydrogen sulfide-exposed stem cells separated from human gingival epithelium, J. Periodontal Res. 48 (3) (2013) 322–330.
[76] S. Li, et al., p53-induced growth arrest is regulated by the mitochondrial SirT3 deacetylase, PLoS One 5 (5) (2010) e10486.
[77] X. Zhao, et al., Berberine attenuates doxorubicin-induced cardiotoxicity in mice, J. Int. Med. Res. 39 (5) (2011) 1720–1727.
[78] G. Hao, et al., Protective effects of berberine against doxorubicin-induced cardiotoxicity in rats by inhibiting metabolism of doxorubicin, Xenobiotica 45 (11) (2015) 1024–1029.
[79] X. Lv, et al., Berberine inhibits doxorubicin-triggered cardiomyocyte apoptosis via attenuating mitochondrial dysfunction and increasing Bcl-2 expression, PLoS One 7 (10) (2012) e47351.
[80] L. Lu, et al., Adriamycin-induced autophagic cardiomyocyte death plays a pathogenic role in a rat model of heart failure, Int. J. Cardiol. 134 (1) (2009) 82–90.
[81] W. Zhu, et al., Acute doxorubicin cardiotoxicity is associated with p53-induced inhibition of the mammalian target of rapamycin pathway, Circulation 119 (1) (2009) 99–106.
[82] Q. Liang, et al., Bioenergetic and autophagic control by Sirt3 in response to nutrient deprivation in mouse embryonic fibroblasts, Biochem. J. 454 (2) (2013) 249–257.
[83] T.E. Rusten, H. Stenmark, p62, an autophagy hero or culprit? Nat. Cell Biol. 12 (3) (2010) 207–209.
[84] G. Kroemer, G. Marino, B. Levine, Autophagy and the integrated stress response, Mol. Cell 40 (2) (2010) 280–293.
[85] J. Zhou, et al., Activation of lysosomal function in the course of autophagy via mTORC1 suppression and autophagosome-lysosome fusion, Cell Res. 23 (4) (2013) 508–523.
[86] S. Aits, M. Jaattela, Lysosomal cell death at a glance, J. Cell Sci. 126 (Pt 9) (2013) 1905–1912.
[87] Y.J. Zhang, et al., Berberine attenuates adverse left ventricular remodeling and cardiac dysfunction after acute myocardial infarction in rats: role of autophagy, Clin. Exp. Pharmacol. Physiol. 41 (12) (2014) 995–1002.
[88] Z. Huang, et al., Berberine alleviates cardiac ischemia/reperfusion injury by inhibiting excessive autophagy in cardiomyocytes, Eur. J. Pharmacol. 762 (2015) 1–10.
[89] R. Ventura-Clapier, A. Garnier, V. Veksler, Transcriptional control of mitochondrial biogenesis: the central role of PGC-1alpha, Cardiovasc. Res. 79 (2) (2008) 208–217.
[90] R.C. Scarpulla, R.B. Vega, D.P. Kelly, Transcriptional integration of mitochondrial biogenesis, Trends Endocrinol. Metab. 23 (9) (2012) 459–466.
[91] X. Kong, et al., Sirtuin 3, a new target of PGC-1alpha, plays an important role in the suppression of ROS and mitochondrial biogenesis, PLoS One 5 (7) (2010) e11707.
[92] T. Zhu, et al., Berberine increases doxorubicin sensitivity by suppressing STAT3 in lung cancer, Am. J. Chin. Med. 43 (7) (2015) 1487–1502.
[93] A. Mittal, S. Tabasum, R.P. Singh, Berberine in combination with doxorubicin suppresses growth of murine melanoma B16F10 cells in culture and xenograft, Phytomedicine 21 (3) (2014) 340–347.